A THEORETICAL FORMULATION FOR FLUTTER ANALYSIS OF A TYPICAL SUBSONIC AIRCRAFT WING (SARAS) USING QUASI-STEADY AERODYNAMIC THEORY

ABSTRACT

A theoretical formulation for flutter analysis has been utilized to develop a working method for determining flutter speed of a typical subsonic aircraft wing. A Galerkin type of analysis has been used to derive the matrix form of equations from the differential equations of motion of the subsonic wing. Quasi-steady aerodynamic theory has been used to model the aerodynamic forces.

A computer code in FORTRAN has been prepared for generation of matrices while the eigen value analysis is performed through MATLAB. The code is benchmarked through the flutter of a rectangular wing. The results from the code agree reasonably with those obtained from the industrial code NASTRAN.

The method is then extended to the flutter analysis of the actual "clean" wing with no control surface effects. The tapered wing is modeled as a stepped assembly of constant section beam elements. Results indicate that the aircraft wing taken is very stiff and therefore is not flutter prone at all in the subsonic regime. To simulate subsonic flutter conditions, a hypothetically reduced stiffness analysis is performed.

In all the cases, the agreement of the results with those of NASTRAN (that uses the Doublet Lattice Method, DLM) indicates the validity of the present method of analysis using the quasi-steady aerodynamic theory, the present work can be extended to study more complicated cases of flutter in the aircraft wing with control surface effects and the T-Tail assembly of aircraft which are expectedly quite prone to subsonic flutter.

ACKNOWLEDGEMENT

I express my sincere thanks to **Dr. A.R.Upadhya**, Director, **Dr. M.N.Sathyanarayana**, Head, Technical Secretariat and **Dr. S.Vishwanath**, Head of Structures Division, NAL, for providing the necessary facilities to carry out my dissertation work at NAL.

I take this opportunity to express my gratitude and indebtedness to **Dr.Somenath Mukherjee**, Scientist, NAL, Bangalore for suggesting this project and keen interest through out the dissertation work. I learnt a lot of physics and mathematics and also how to work independently from him.

I wish to express heartfelt gratitude to **Dr. D.L.Prabhakara**, Professor, Department of Civil Engineering, Malnad College of Engineering, Hassan for his excellent guidance during the course of this dissertation work.

I wish to thank **Smt Manju** and **Smt Swarnalatha**, Scientists, NAL, Bangalore for their extended help during this project work.

I express my profound sense of gratitude to **Dr.D.L.Manjunath**, Professor and Head, Department of Civil Engineering, Malnad College of Engineering, Hassan for allowing me to do this dissertation work in NAL, Bangalore and for his valuable suggestions and advice.

I am thankful to **Dr. Karisiddappa**, Professor, PG coordinator M.Tech [CADS] Dept. of Civil Engineering**, Dr. K.Munjunath**, Assistant Professor and **Dr. M.S.Kalappa,** Assistant Professor, Dept. of Civil Engineering Department, Malnad College of Engineering, Hassan, for their constant support through the course.

I am also grateful to my **Sister** and my **Parents** for their constant support.

CHAPTER-1.

INTRODUCTION

1.1 Aeroelasticity

Aero elasticity is the study of the effect of the aerodynamic forces on elastic bodies. If in the analysis of any structural dynamic systems aerodynamic loading is included then the resulting dynamic phenomenon may be classified as Aeroelastic.

The classical theory of elasticity deals with the stress and deformation of an elastic body under prescribed external forces or displacements. The external loading acting on the body is, in general, independent of the deformation of the body. It is usually assumed that the deformation is small and does not substantially affect the action of external forces. In such a case, we often neglect the changes in dimensions of the body and base our calculations on the initial shape.

The situation is different, however, in most problems of aero elasticity. The aerodynamic forces depend critically on the attitude of the body relative to the flow. The elastic deformation plays an important role in determining the external loading itself. The magnitude of the aerodynamic force is not known until the elastic deformation is determined. In general, therefore, the external load is

not known until the problem is solved. Aero elastic phenomena have a significant influence on the design of flight vehicles.

1.2 Aeroelastic flutter

One of the interesting problems in aeroelasticity is the stability (or rather instability) of structure in wind. Since, for a given configuration of the elastic body, the aerodynamic force increases rapidly with the wind speed, while elastic stiffness is independent of the wind, there may exist a critical wind speed at which the structure becomes dynamically unstable. Such dynamic instability may cause excessive oscillatory deformations that increase in amplitude exponentially with time, and may lead to the destruction of the structure.

A major problem is the flutter of structures such as airplanes or suspension bridges, when small disturbances of an incidental nature induce more or less violent oscillations. It is characterized by the interplay of aerodynamic, elastic and inertia forces and is called a problem of dynamic aeroelastic instability. The particular case of an oscillation with zero frequency, in which in general the inertia force is neglected, is called the steady state, or static aeroelastic instability.

There is a close relationship between the stability problems and the response problems. Mathematically, most stability problems can be described by a system of homogenous equations, which are satisfied by a trivial solution of zero displacement or zero motion, meaning that nothing happens at all. On the other hand, a response

problem is represented by a nonhomogenous system; i.e., the initial conditions and the external forces are such as to cause the governing equations to be nonhomogenous, and to admit a solution not vanishing identically.

A response problem generally associates with a stability problem. As an example, consider the response of an airplane wing to atmospheric turbulences. We can formulate the problem of flutter by asking the following questions: is there a critical speed of flight at which the airplane structure becomes exceedingly sensitive to the atmospheric turbulence; i.e., does there exist a speed at which the structure may have a motion of finite amplitude, even in the limiting case of an atmospheric turbulence of zero intensity? This is equivalent to the following formulation, which is usually made in flutter analysis: Is there a critical speed at which the aeroelastic system becomes neutrally stable, at which motion of the structure is possible without any external excitation?

Thus the response of the airplane structure to the atmospheric turbulence and the flutter problem are linked together. When the response of the structure to a finite disturbance is finite, the structure is stable, and flutter will not occur. When the structure flutters at a critical speed of flow, its response to a finite disturbance becomes indefinite.

1.3 Literature review

The earliest study of flutter seems to have been made by Lanchester [1], Bairstow and Fage [2] in 1916. In 1918, Blasius [3] made some calculations after the failure of the lower wing of Albatross D3 biplane. But the real development of the flutter analysis had to wait for the development of Non-stationary airfoil theory by Kutta and Joukowsky.

Glauret [4,5] published data on the force and moment acting on a cylindrical body due to an arbitrary motion. In 1934, Theodorsen's [6] exact solution of a harmonically oscillating wing with a flap was published.

The torsion flutter was first found by Glauret in 1929. It is discussed in detail by Smilg [7]

Several types of single degree of freedom flutter involving control surfaces at both subsonic and supersonic speeds have been found [8,9], all requiring the fulfillment of certain special conditions on the rotational axis locations, the reduced frequency and the mass moment of inertia.

Pure bending flutter is possible for a cantilever swept wing if it is heavy enough relative to the surrounding air and has a sufficiently large sweep angle [10].

The stability of more complicated motions can be determined by calculating the energy input from the airstream. The bending torsion case in an incompressible fluid has been calculated by J.H.Greidanus and the energy coefficient in Bending-Torsion oscillations has been given [11]

The use of 'Quasi-steady' Aerodynamic theory for the flutter analysis of the wings and excellent treatises in the field of aeroelasticity are given by Y.C.Fung [12], E.H.Dowell [13,14], L.Mirovitch [15] and others.

In the typical wing whose elastic axis (locus of shear centers) and mass axis (locus of center of gravity) do not coincide, the nature of oscillations is always coupled flexure-torsion. A vast literature exists on the flexure-torsion problem of engineering structures. Evins [16] has given comprehensive details about vibration fixture transducers and instrumentation. Bisplinghoff and H.Ashley [17] has described the elastic characteristics shape and inertial idealization.

A new method for determining mass and stiffness matrices from modal test data is described by Alvin and Paterson [18]. This method determines minimum order mass and stiffness matrices, which is used to determine the optimum sensor location. Dugundji [19] examined panel flutter and the rate of damping. The problem of two and three-dimensional plate undergoing cyclic oscillations and aeroelastic instability is investigated by Dowell [13,14].

The behavior of tip loaded cantilever beam with an arbitrary cross section using a power series solution technique for the out of plane flexure and torsion case is discussed by Kosmataka [20]. This includes a linear relation developed for locating shear center. Abott [21] has suggested a technique for representing the shape of the aerofoil through analytical relations.

The coupled flexure-torsion vibration response of beam under deterministic and random load is investigated thoroughly by Eslimy and Sobby [22] by use of normal mode method. The exact determination of coupled flexure-torsion vibration characteristics of uniform beam having single cross section symmetry is studied by Dokumaci [23].

Literature in the context of excitation systems and design of electromagnets is referred to by Chatterji [24] and Wilson [25]. Haisler and Allen [26] and Kuhn [27] have described a procedure of computing required centroidal and elastic properties including shear flows. Mathematical formulations of flexure-torsion problem have been broadly described by Mirovitch [15], Thomson [28], Hurty and Rubinstein [29] and Y.C.Fung [12]. Talukedar, Kamle and Yadav [30] have discussed an analytical method for flexure-torsion coupled vibration of vehicles leading to aircraft application.

At present, subsonic flight is a daily event and supersonic and hypersonic flights are a reality. Now aeroelastic analysis has become an organic part of the design.

1.4 Summary of the present work

The present work involves the flutter analysis of a typical low speed subsonic aircraft wing using a beam model as an idealized structure representing the same. A Galerkin type of analysis using normal mode superposition is adopted for the solution of the differential equations of motion. Free vibration analysis of the wing is carried out using the elementary beam model. Subsequently, the flutter analysis of the aircraft wing is carried out using the elementary beam model and quasi-steady aerodynamic theory, and the flutter speed is compared with that obtained from NASTRAN. Provision is made to account for dynamic coupling between the bending and torsional degrees of freedom due to the fact that the shear center can be off the centroidal axis for beams of unsymmetric sections.

As a benchmark problem, free vibration analysis of a cantilever beam of a typical uniform rectangular section is chosen. The NASTRAN results are generated using beam elements. Good agreement between the results can be observed.

A typical subsonic (SARAS) aircraft wing (clean wing, with no control surface effects) is then analysed using the program code. The generated data for the elastic and inertial properties of the wing, discretized as a collection of stepped beam elements, is employed for the free vibration analysis and also the flutter analysis. These are then compared with the results obtained from NASTRAN.

For the “clean” wing analysis for the SARAS aircraft, it is found that the flutter speed is beyond the subsonic regime.i.e, it indicates the wing does not flutter in the subsonic flow. Even for the case of a flutter speed (determined by the present subsonic formulation and NASTRAN code) that exceeds the limit of subsonic regime, agreement of the results show that the computational procedure adopted here is reasonably reliable. As a check, results are generated with reduced stiffness parameters so that the flutter speed effectively falls in the subsonic regime. Again results agree with those from NASTRAN, showing the validity of the present method of analysis.

CHAPTER -2

MATHEMATICAL FORMULATIONS

In this chapter, the mathematical formulation of subsonic flutter analysis of a typical subsonic wing is presented. For low speed subsonic aircrafts, the wings are usually unswept or the sweep angle will usually be very small. A typical subsonic wing is shown in Fig 2.1 and a typical uniform rectangular wing is shown in Fig 2.2 For aerodynamic reasons, a typical low speed subsonic wing is characterized by high aspect ratio (span / mean chord) and a straight or nearly straight configuration. This fact is advantageous for structural analysis of the wing using a simple beam model, despite the complex arrangement of the constituent structural elements. An airplane wing, as an elastic body, has infinitely many degrees of freedom. But owing to its particular construction, its elastic deformation in any chord wise section can usually be described with sufficient accuracy by two quantities: the deflection at a reference point, and the angle of rotation about that point, i.e., the flexural and torsional deformations respectively.

Each wing is assumed to behave like a cantilever, supported at the axis of connectivity of the two wings, inside the fuselage. The wing is visualized as a collection of stepped beam elements, each having its respective elastic properties. A modal analysis method is used, using the classical cantilever modes of beams. The present analysis is limited to the “clean wing”, i.e., the ailerons are not involved in the analysis.

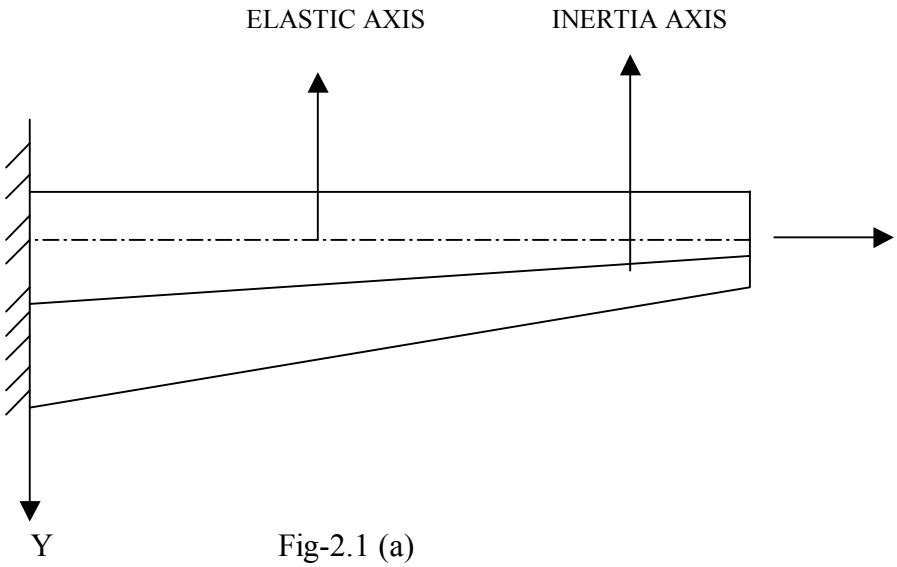

Fig-2.1 (a)

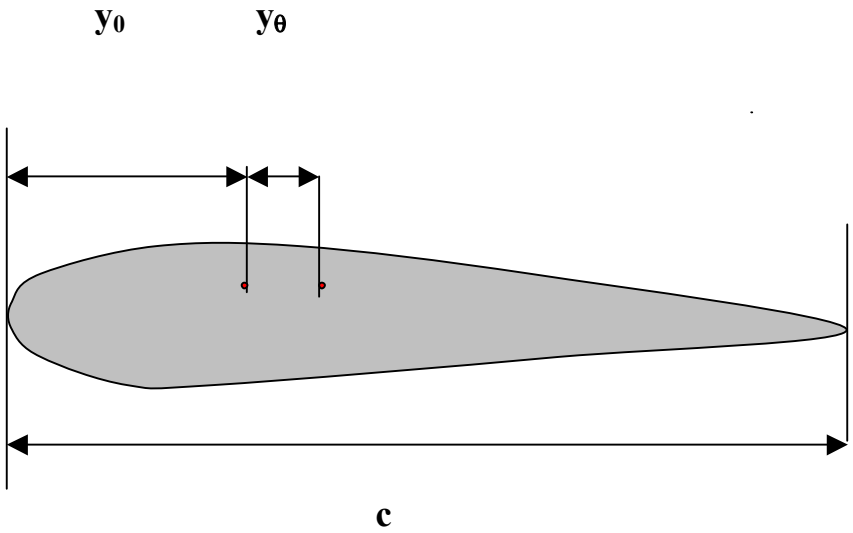

Fig-2.1 (b)

Fig-2.1 (a) A typical subsonic wing

Fig-2.1 (b) A typical aerofoil section

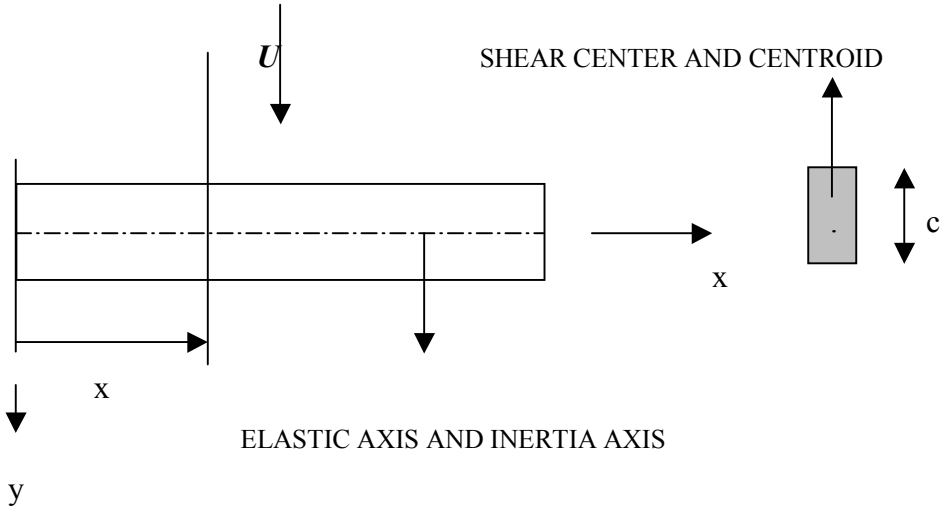

Fig-2.2 (a) Fig-2.2 (b)

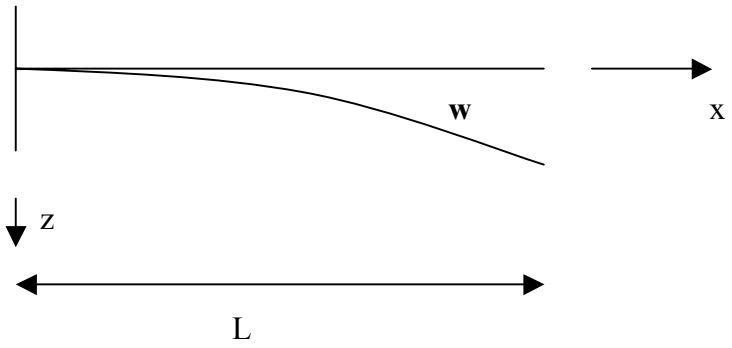

Fig-2.2(c)

Fig-2.2 (a) A typical uniform wing

Fig-2.2 (b) Section of the uniform wing

Fig-2.2 (c) Deflection of the uniform wing

2.1 Formulation of equations of motion:

An unswept cantilever wing having a straight elastic axis perpendicular to the fuselage, which is assumed to be fixed in space is considered. The wing deformation can be measured by a deflection 'w' and a rotation 'θ' about the elastic axis, w being positive downward and θ is assumed positive if the leading edge up. The chordwise displacement will be neglected. The frame of reference is chosen as shown in Fig 2.1 (a). with the x-axis coinciding with the elastic axis. Let y_θ be the distance between the center of mass and the elastic axis at any section, positive if the former lies behind the latter. Let c be the chord length and y_o be the distance of the elastic axis after the leading edge. In a steady flow of speed *U*, the wing will have some elastic deformation, which is however, of no concern to the problem of flutter. In the following, the free motion of the wing following an initial disturbance is considered.

Thus let 'w' and 'θ' be the deviations from the equilibrium state, and let the inertia, elastic and aerodynamic forces correspond also to the deviations from the steady-state values; then, for small disturbances, the principle of superposition holds, and we have the following equations of motion.

$$\frac{\partial^2}{\partial x^2}\left(EI\frac{\partial^2 w}{\partial x^2}\right)+m\frac{\partial^2 w}{\partial t^2}+my_\theta\frac{\partial^2 \theta}{\partial t^2}+L=0 \qquad \text{--------- (2.1)}$$

$$-\frac{\partial}{\partial x}\left(GJ\frac{\partial \theta}{\partial x}\right)+I_\theta\frac{\partial^2 \theta}{\partial t^2}+my_\theta\frac{\partial^2 w}{\partial t^2}+M=0 \qquad \text{---------- (2.2)}$$

where EI and GJ are the bending and torsional rigidity of the wing, m and I_θ are the mass and mass moment of inertia about the elastic axis of the wing section at x, per unit length along the span, and L and M are the aerodynamic lift and moment per unit span, respectively,

where,

$$L=\frac{\rho U^2}{2}cC_L \qquad \text{---------- (2.3)}$$

$$M=\frac{\rho U^2}{2}c^2C_M=\frac{\rho U^2}{2}c^2\left[(C_M)_{LE}+\frac{x_0}{c}C_L\right] \qquad \text{---------- (2.4)}$$

in which the lift and moment coefficients are given by the quasi-steady subsonic aerodynamic theory as

$$C_L=\frac{dC_L}{d\theta}\left[\theta+\frac{1}{U}\frac{dh}{dt}+\frac{1}{U}\left(\frac{3}{4}c-x_0\right)\frac{d\theta}{dt}\right] \qquad \text{---------- (2.5)}$$

$$(C_M)_{l.e.}=-\frac{c\pi}{8U}\frac{d\theta}{dt}-\frac{1}{4}C_L \qquad \text{---------- (2.6)}$$

The aerodynamic forces and moments are obtained by using the quasi-steady 'strip theory', whereby local lift coefficient is proportional to the instantaneous angle of attack θ. The derivative $dC_L/d\theta$ is considered to be constant, with a theoretical value of 2π for incompressible flow and an experimental value of somewhat less than 2π. Moreover the aerodynamic analysis is subject to the quasi-steady assumption, which implies that only the instantaneous deformation is important and the history of motion may be neglected.

Equations 2.5 and 2.6 give the lift and moment for variable w and θ.

From these equations we get,

$$\frac{\partial^2}{\partial x^2}\left(EI\frac{\partial^2 w}{\partial x^2}\right)+m\frac{\partial^2 w}{\partial t^2}+my_\theta\frac{\partial^2\theta}{\partial t^2}+\frac{\rho U^2}{2}c\frac{dC_L}{d\theta}\left[\theta+\frac{1}{U}\frac{\partial w}{\partial t}+\frac{c}{U}\left(\frac{3}{4}-\frac{y_0}{c}\right)\frac{\partial\theta}{\partial t}\right]=0$$

$$0<x<L$$

$$-\frac{\partial}{\partial x}\left(GJ\frac{\partial\theta}{\partial x}\right)+my_\theta\frac{\partial^2 w}{\partial t^2}+I_\theta\frac{\partial^2\theta}{\partial t^2}-\frac{\rho U^2}{2}c^2$$

$$\left\{-\frac{c\pi}{8U}\frac{\partial\theta}{\partial t}+\left(\frac{y_0}{c}-\frac{1}{4}\right)\frac{dC_L}{d\theta}\left[\theta+\frac{1}{U}\frac{\partial w}{\partial t}+\frac{c}{U}\left(\frac{3}{4}-\frac{y_0}{c}\right)\frac{\partial\theta}{\partial t}\right]\right\}=0$$

$$0<x<L$$

---------- (2.7) and (2.8)

The displacements ‘w’ and ‘θ’ are subject to the Boundary conditions

$$w = \frac{\partial w}{\partial x} = \theta = 0 \qquad \text{at x=0}$$

$$\frac{\partial^2 w}{\partial x^2} = \frac{\partial^3 w}{\partial x^3} = \frac{\partial \theta}{\partial x} = 0 \qquad \text{at x= L} \qquad \text{---------- (2.9)}$$

Should y_θ and U be zero, Eqs (2.7) and (2.8) would be reduced to two independent equations, one for w and one for θ. The terms involving y_θ and U indicate inertia and aerodynamic couplings.

Since Eqs (2.7) and (2.8) are linear equations with constant coefficients, the solution can be written in the usual form

$$w(x,t) = W(x)e^{\lambda t} \qquad \theta(x,t) = \Theta(x)e^{\lambda t}$$

--------- (2.10)

where λ is generally complex. Introducing Eq. (2.10) into Eqs (2.7) and (2.8) and dividing through out by $e^{\lambda t}$, we obtain the ordinary differential equations

$$\left(EIW''\right)'' + \frac{\rho U^2}{2} c \frac{dC_L}{d\theta}\Theta + \lambda \frac{\rho U}{2} c \frac{dC_L}{d\theta}\left[W + c\left(\frac{3}{4} - \frac{y_0}{c}\right)\Theta\right] + \lambda^2 m(W + y_\theta \Theta) = 0$$

---------(2.11a)

$$-\left(GJ\Theta'\right)' - \frac{\rho U^2}{2} c^2 \left(\frac{y_0}{c} - \frac{1}{4}\right)\frac{dC_L}{d\theta}\Theta - \lambda \frac{\rho U}{2}$$
$$c^2 \left\{\left(\frac{y_0}{c} - \frac{1}{4}\right)\frac{dC_L}{d\theta}W + c\left[\left(\frac{y_0}{c} - \frac{1}{4}\right)\left(\frac{3}{4} - \frac{y_0}{c}\right)\frac{dC_L}{d\theta} - \frac{\pi}{8}\right]\Theta\right\} +$$
$$\lambda^2 \left(m y_\theta W + I_\theta \Theta\right) = 0$$

----------(2.11b)

where $(\ )' = \frac{d}{dx}(\ )$ and $(\ )'' = \frac{d^2}{dx^2}(\ )$

The boundary conditions retain the same form except that w and θ are replaced by W and Θ, respectively and partial derivatives of w and θ with respect to x by total derivatives.

No closed form solution of equations (2.11) is possible; hence an approximate solution is used. Before proceeding with the solution, however, it will prove instructive to examine the effect of airflow speed U on the parameter λ that gives the stability condition of the system.

2.2 Free vibration analysis of the wing

Free vibration analysis of the wing is performed using the Euler beam model with the help of computer code as explained earlier. Good agreement between the results confirms the validity of the present beam model and the relevant computer code. The natural frequencies of the equivalent beam model for one wing are determined by this code and compared with NASTRAN.

In the beam formulation, the shear center offset from the centroid brings about dynamic coupling between the bending and torsional modes. This coupling is obvious from the bending and torsional modes. No pure torsion and bending modes exist in the structure.

For U = 0(free vibration), the above equations reduce to,

$$\left(EIW''\right)'' + \lambda^2 m\left(W + y_\theta \Theta\right) = 0 \qquad 0 < x < L \qquad \text{---------(2.12a)}$$

$$-\left(GJ\Theta'\right)' + \lambda^2\left(my_\theta W + I_\theta \Theta\right) = 0 \qquad 0 < x < L \qquad \text{--------- (2.12b)}$$

The system can be shown to be self-adjoint and positive definite.

Using Galerkin's method and assuming solution

$$W = \sum_{j=1}^{n} a_j \phi_j \qquad \Theta = \sum_{j=n+1}^{n+m} a_j \phi_j \qquad \text{----------(2.13)}$$

where ϕ_j are the modal functions, which should satisfy the boundary conditions as shown before.

The independent pure bending modes and pure torsional modes of the uniform cantilever beam with symmetric sections (zero shear center offset) are suitable modal functions.

Pure j^{th} beam bending mode for the classical Euler beam with cantilever boundary condition is given as [34]

$$\phi_j = (\cosh a_n x - \cos a_n x) - \sigma_n (\sinh a_n x - \sin a_n x) \quad j=1,2...n$$

------- (2.14a)

where, $\sigma_n = \dfrac{(\cosh a_n L - \cos a_n L)}{(\sinh a_n L - \sin a_n L)}$

Cantilever boundary conditions satisfied are

$$\phi_j(x=0)=0 \qquad \phi_j'(x=0)=0 \qquad j=1,2,3.....n$$

The wave number a_n can be computed so as to satisfy the characteristic equation,

$$\cos(a_n L).\cosh(a_n L)+1=0$$

Pure j [th] torsional mode of the uniform beam is

$$\phi_j=\sin\left(\frac{2k-1}{2L}\pi\right)x \qquad j = n+k\ ;\ k = 1,2,3...m$$

----------(2.14b)

The boundary conditions satisfied here are

$$\phi_j(x=0)=0 \qquad j=n+1,n+2.....n+m$$

$$\phi_j'(x=L)=0$$

Introducing Eqs. (2.13) Into Eqs. (2.12)

$$\sum_{j=1}^{n} a_j\left(EI\phi_j''\right)''+\lambda^2\sum_{j=1}^{n} a_j m\phi_j+\lambda^2\sum_{j=n+1}^{n+m} a_j m y_\theta\phi_j=0 \qquad \text{----------(2.15a)}$$

$$-\sum_{j=n+1}^{n+m} a_j\left(GJ\phi_j'\right)'+\lambda^2\sum_{j=1}^{n} a_j m y_\theta\phi_j+\lambda^2\sum_{j=n+1}^{n+m} a_j I_\theta\phi_j=0 \text{ -------(2.15b)}$$

Multiplying equation (2.15a) by ϕ_i (I=1,2…n) and equation (2.15b) by ϕ_i (i=n+1,n+2,…n+m), and integrating both results over the interval $0 \le x \le L$ we obtain algebraic Eigen value problem

$$\sum_{j=1}^{n+m} k_{ij} a_j + \lambda^2 \sum_{j=1}^{n+m} m_{ij} a_j = 0 \qquad \text{(i=1,2…n+m)} \quad \text{-------(2.16)}$$

where for the n bending modes alone

$$k_{ij} = \int_0^L \phi_i \left(EI \phi_j'' \right)'' dx = \int_0^L EI \phi_i'' \phi_j'' dx = k_{ij}$$

(i, j = 1,2…n) …….(2.17a)

Orthogonality of Normal modes yields the condition

$$k_{ij} = 0 \qquad \text{for} \quad i \neq j$$

and for the torsional modes alone,

$$k_{ij} = -\int_0^L \phi_i \left(GJ \phi_j' \right)' dx = \int_0^L GJ \phi_i' \phi_j' dx = k_{ji}$$

i, j = n + 1, n + 2,…...n + m

-------(2.17b)

Again $k_{ij} = 0$ for $i \neq j$ is the orthogonality condition

and

$$m_{ij} = m_{ji} = \int_0^L m\phi_i\phi_j dx \qquad \text{i , j = 1,….n}$$

--------(2.17c)

$$m_{ij} = m_{ji} = \int_0^L my_\theta\phi_i\phi_j dx \qquad \text{i = 1,2,…n; j = n+1,n+2,...n+m}$$

$$m_{ij} = m_{ji} = \int_0^L I_\theta\phi_i\phi_j dx \qquad \text{i , j = n + 1, n + 2,…...n + m}$$

---------(2.17d)

Orthogonality condition $m_{ij} = 0$ for $i \neq j$

These are the symmetric stiffness and mass coefficients. Equation (2.16) can be written in the matrix form

$Ka = -\lambda^2 Ma$ ----------(2.18)

where K and M are positive definite symmetric matrices. Hence, the eigenvalue $-\lambda^2$ must be real and positive, the square root of which yields the natural circular frequency (rad/sec), {i.e., $\omega_i = \sqrt{-\lambda_i^2}$ for i^{th} mode}

2.3 Flutter analysis of the wing:

Flutter analysis of the wing is also carried out using the same elementary beam model**.** The quasi-steady aerodynamic theory is used to obtain the aerodynamic forces interacting with the structure. First the problem is solved taking one bending mode and one torsion mode as a first estimate and then the result has been improved taking higher modes. The same is solved in NASTRAN in *pk*-method. The results obtained in NASTRAN matches the results obtained through the code. The flutter speed obtained through the code has shown conservative values.

The flutter speed obtained for the present configuration has shown to be very high and also that the wing is very stiff. Hence the stiffness of the wing is reduced by reducing the modulus of elasticity and correspondingly the modulus of rigidity. The results obtained for the wing with reduced stiffness parameters are typical for subsonic flutter.

The eigenvalue λ is a continuous function of the air speed U. When U is not zero, but infinitesimally small, the exponent λ is no longer pure imaginary but complex, $\lambda = \alpha + i\omega$. Of course, to investigate this case, we must return to the non-self adjoint system. It can be shown that for sufficiently small U and for $(dC_L / d\theta) < 2\pi$, the wing is losing energy to the surrounding air, so that the motion is damped oscillatory, and hence asymptotically stable. The clear implication is that α is negative. As U increases, α can become

positive, so that at the point at which α changes sign, the motion ceases to be damped oscillatory and becomes unstable. The air speed corresponding to $\alpha = 0$ is known as critical speed and denoted by Ucr. There are many critical values of U but, because in actual flight U increases from an initially zero value, the lowest critical value is the most important. One can distinguish between two critical cases, depending on the value of ω. When $\alpha = 0$ and $\omega = 0$ the wing is said to be in critical divergent condition. When $\alpha = 0$ and $\omega \neq 0$ the wing is said to be in critical flutter condition.

The above qualitative discussion can be substantiated by a more quantitative analysis. To this end, we must derive and solve the complete non-self adjoint eigenvalue problem. Introducing solution (2.13) into Eqs.(2.11), multiplying Eq. (2.11a) by ϕ_i (i = 1,2…n) and Eq. (2.11b) by ϕ_i (i = n+1,n+2…..n+m) and integrating both results over the interval $0 < x < L$, we obtain the eigenvalue problem

$$[K + U^2H + \lambda UL + \lambda^2 M] a = 0 \qquad \text{----------(2.19)}$$

The matrices H and L are not symmetric. Their elements can be shown to have the expressions

$$h_{ij} = 0 \qquad i, j = 1, 2, ...n$$

$$h_{ij} = \frac{\rho}{2}\frac{dC_L}{d\theta}\int_0^L c\phi_i\phi_j dx \qquad i = 1, 2, ...n;\ j = n+1, n+2, ...n+m$$

$$h_{ij} = 0 \qquad i = n+1, n+2, ...n+m;\ j = 1, 2, ...n$$

$$h_{ij} = -\frac{\rho}{2}\frac{dC_L}{d\theta}\int_0^L c^2\left(\frac{y_0}{c} - \frac{1}{4}\right)\phi_i\phi_j dx \quad i, j = n+1, n+2, ...n+m$$

----------.(2.20a)

$$l_{ij} = \frac{\rho}{2}\frac{dC_L}{d\theta}\int_0^L c\phi_i\phi_j dx \qquad i, j = 1, 2, ...n$$

$$l_{ij} = \frac{\rho}{2}\frac{dC_L}{d\theta}\int_0^L c^2\left(\frac{3}{4} - \frac{y_0}{c}\right)\phi_i\phi_j dx \qquad i = 1, 2, ...n$$

$$j = n+1, n+2, ...n+m$$

$$l_{ij} = -\frac{\rho}{2}\frac{dC_L}{d\theta}\int_0^L c^2\left(\frac{y_0}{c} - \frac{1}{4}\right)\phi_i\phi_j dx \qquad i = n+1, n+2, ...n+m\ ;$$

$$j = 1, 2, ...n$$

$$l_{ij} = \frac{\rho}{2}\int_0^L c^3\left[\frac{\pi}{8} - \left(\frac{y_0}{c} - \frac{1}{4}\right)\left(\frac{3}{4} - \frac{y_0}{c}\right)\frac{dC_L}{d\theta}\right]\phi_i\phi_j dx$$

$$i, j = n+1, n+2, ...n+m \qquad \text{----------(2.20b)}$$

Using the same procedure, we can reduce the eigenvalue problem to the standard form

$$k^* a^* = \lambda M^* a^* \qquad \ldots\ldots(2.21)$$

where

$$a^* = \begin{bmatrix} a^T & b^T \end{bmatrix}^T = \begin{bmatrix} a^T & \lambda a^T \end{bmatrix}^T \qquad \ldots\ldots(2.22)$$

is a 2 (n + m) vector and

$$K^* = \begin{bmatrix} 0 & 1 \\ -\left(K + U^2 H\right) & -UL \end{bmatrix}$$

$$M^* = \begin{bmatrix} 1 & 0 \\ 0 & M \end{bmatrix} \qquad (2.23\ a, b)$$

are 2 (n + m) x 2 (n + m) matrices.

The critical value U_{cr} of interest here is the lowest value of U for which

$$\alpha = \mathrm{Re}\,\lambda = 0$$

Flutter occurs if the real part of the eigenvalue i.e., $\alpha = \mathrm{Re}\lambda > 0$ and the imaginary part of the eigenvalue i.e., $\omega = I_m(\lambda) \neq 0$

For $\alpha > 0$ and $\omega = 0$, divergence occurs.

The characteristic behavior of a typical mode that undergoes flutter instability under varying airflow speeds U is shown in Fig.2.3

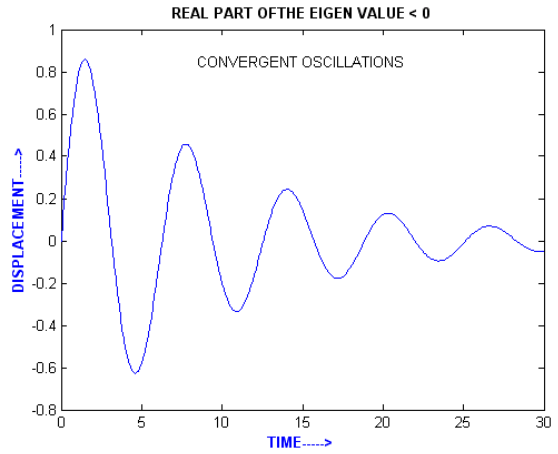

Stable

$U<U_{cr}$

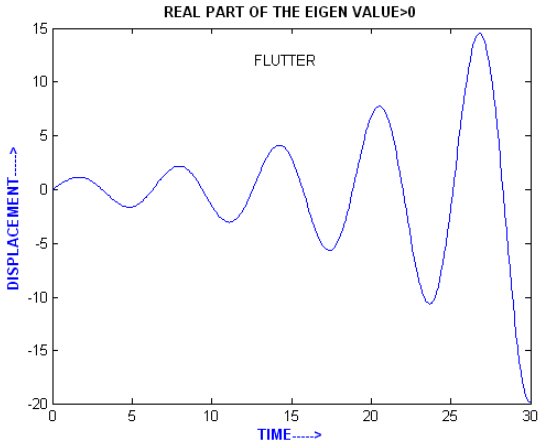

Unstable (Flutter)

$U>U_{cr}$

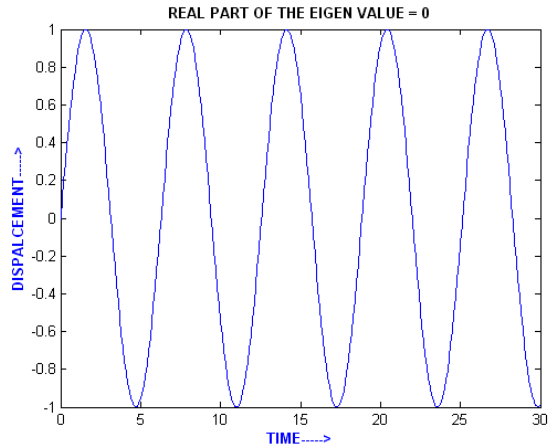

Flutter boundary

$U=U_{cr}$

Fig 2.3 Behavior of typical mode amplitude when imaginary part ≠ 0

To compute U_{cr}, one must solve the eigenvalue problem repeatedly for increasing values of U. For small values of U, all the eigen values $\lambda_r\,(r=1,2,.....,2n+2m)$ have negative real parts. The first value of u at which the real part of an eigenvalue reduces to zero is U_{cr}.

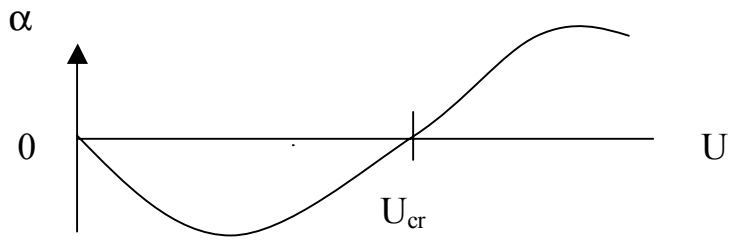

A first estimate of Ucr can be obtained by approximating W and Θ by means of a single term, $n=m=1$. Then, letting λ = iω, U_{cr} is the value of U, which permits the solution of the determinantal equation

$$\det\begin{bmatrix} i\omega & 0 & -1 & 0 \\ 0 & i\omega & 0 & -1 \\ k_{11} & U^2h_{12} & i\omega m_{11}+Ul_{11} & i\omega m_{12}+Ul_{12} \\ 0 & k_{22}+U^2h_{22} & i\omega m_{12}+Ul_{21} & i\omega m_{22}+Ul_{22} \end{bmatrix}=0$$

---------- (2.24)

Equation (2.24) yields

$$\omega^4\left(m_{11}m_{22}-m_{12}{}^2\right)-i\omega^3U\left[m_{11}l_{22}+m_{22}l_{11}-m_{12}\left(l_{12}+l_{21}\right)\right]$$
$$-\omega^2\left[U^2\left(l_{11}l_{22}-l_{12}l_{21}-h_{12}m_{12}+h_{22}m_{11}\right)+k_{22}m_{11}+k_{11}m_{22}\right]$$
$$-i\omega U\left[U^2\left(h_{12}l_{21}+h_{22}l_{11}\right)+k_{22}l_{11}-k_{11}l_{22}\right]+k_{11}\left(U^2h_{22}+k_{22}\right)=0$$

----------(2.25)

Equating the imaginary part to zero, we obtain

$$\omega^2=\frac{U^2\left(h_{12}l_{21}+h_{22}l_{11}\right)+k_{22}l_{11}-k_{11}l_{22}}{m_{12}\left(l_{12}+l_{21}\right)-m_{11}l_{22}+m_{22}l_{11}}$$

so that substituting into the real part of Eq. 19, we can write the quadratic equation in U^2

$$AU^4+BU^2+C=0$$

----------(2.26)

where,

$$A=\left(h_{12}l_{21}+h_{22}l_{11}\right)$$
$$\left\{\begin{array}{l}\left(h_{12}l_{21}+h_{22}l_{11}\right)\left(m_{11}m_{22}-m_{12}{}^2\right)-\left(l_{11}l_{22}-l_{12}l_{21}-h_{12}m_{12}+h_{22}m_{11}\right)\\ \left[m_{12}\left(l_{12}+l_{21}\right)-\left(m_{11}l_{22}+m_{22}l_{11}\right)\right]\end{array}\right\}$$

$$B = 2\left(h_{12}l_{21} + h_{22}l_{11}\right)\left(k_{22}l_{11} - k_{11}l_{22}\right)\left(m_{11}m_{22} - m_{12}{}^2\right)$$
$$-\left[\left(h_{12}l_{21} + h_{22}l_{11}\right)\left(k_{22}m_{11} + k_{11}m_{22}\right) + \left(k_{22}l_{11} - k_{11}l_{22}\right)\left(l_{11}l_{22} - l_{12}l_{21} - h_{12}m_{12} + h_{22}m_{11}\right)\right]$$
$$\left[m_{12}\left(l_{12} + l_{21}\right) - \left(m_{11}l_{22} + m_{22}l_{11}\right)\right]$$
$$+k_{11}h_{22}\left[m_{12}\left(l_{12} + l_{21}\right) - \left(m_{11}l_{22} + m_{22}l_{22}\right)\right]^2$$

$$C = \left(k_{22}l_{11} - k_{11}l_{22}\right)^2\left(m_{11}m_{22} - m_{12}{}^2\right) - \left(k_{22}l_{11} - k_{11}l_{22}\right)$$
$$\left(k_{22}m_{11} + k_{11}m_{22}\right)\left[m_{12}\left(l_{12} + l_{21}\right) - \left(m_{11}l_{22} + m_{22}l_{11}\right)\right]$$
$$+k_{11}k_{22}\left[m_{12}\left(l_{12} + l_{21}\right) - \left(m_{11}l_{22} + m_{22}l_{11}\right)\right]^2$$

The solution of Eq. (2.26) is

$$U^2 = -\frac{B}{2A} \pm \frac{1}{2A}\sqrt{B^2 - 4AC} \qquad \text{----------(2.27)}$$

The first estimate of the critical value U_{cr} is the smallest positive value of U that can be obtained.

2.4 Discretization and integration for tapered wing (SARAS)

A typical aircraft wing (SARAS) is actually tapered along the length. Thus, the elastic rigidity, inertia loading and aerodynamic chord length distributions are not uniform.

To include the effects of varying section properties, the following scheme of discretization and integration is adopted, but using global modal functions ϕ_i, satisfying cantilever boundary conditions [equations (2.14 a, b)]

The entire wing of length L is discretized into, say, N elements. For element r of length l_r, the elastic rigidities $(EI)_r$ and $(GJ)_r$, mass per unit lengths m_r and average chord c_r are assumed to be constant within the element.

Therefore integrals in equations (2.17) and (2.20) are approximated by the following expressions

Bending:

$$k_{ij} = \int_0^L EI\phi_i''\phi_j'' dx \approx \sum_{r=1}^{N} (EI)_r \int_{x_r}^{x_{r+1}} \phi_i''\phi_j'' dx$$

$$m_{ij} = \int_0^L m\phi_i\phi_j dx \approx \sum_{r=1}^{N} m_r \int_{x_r}^{x_{r+1}} \phi_i\phi_j dx \qquad i, j = 1, 2, 3.....n$$

----------(2.28)

Torsion:

$$k_{ij} = \int_0^L GJ\phi_i'\phi_j' dx \approx \sum_{r=1}^{N} (GJ)_r \int_{x_r}^{x_{r+1}} \phi_i'\phi_j' dx$$

$$m_{ij} = \int_0^L I_\theta \phi_i \phi_j dx \approx \sum_{r=1}^{N} (I_\theta)_r \int_{x_r}^{x_{r+1}} \phi_i \phi_j dx$$

$$i, j = n+1, n+2.....n+m$$

---------- (2.29)

Coupled inertia:

$$m_{ij} = \int_0^L m y_\theta \phi_i \phi_j dx \approx \sum_{r=1}^{N} m_r y_{\theta r} \int_{x_r}^{x_{r+1}} \phi_i \phi_j dx \qquad i = 1, 2.....n$$

$$j = n+1, n+2.....n+m$$

---------(2.30)

The aerodynamic parameters of equations (2.20) can be likewise obtained by piecewise integrations, where

$$\int_0^L c\phi_i\phi_j dx \approx \sum_{r=1}^{N} c_r \int_{x_r}^{x_{r+1}} \phi_i\phi_j dx$$

$$\int_0^L c^2\left(\frac{y_0}{c}-\frac{1}{4}\right)\phi_i\phi_j dx \approx \sum_{r=1}^{N} c_r^2\left[\frac{(y_0)_r}{c_r}-\frac{1}{4}\right]\int_x^{x_{r+1}} \phi_i\phi_j dx$$

and

$$\int_0^L c^3\left[\frac{\pi}{8}-\left(\frac{y_0}{c}-\frac{1}{4}\right)\left(\frac{3}{4}-\frac{y_0}{c}\right)\frac{dl_L}{d\theta}\right]\phi_i\phi_j dx \approx \sum_{r=1}^{N} c_r^3\left[\frac{\pi}{8}-\left(\frac{y_{0r}}{c_r}-\frac{1}{4}\right)\left(\frac{3}{4}-\frac{y_{0r}}{c_r}\right)\right]\int_{x_r}^{x_{r+1}} \phi_i\phi_j dx$$

---------- (2.31)

These expressions are substituted in the eqn. (2.19) for flutter analysis of tapered beam

The chord length of the wing is assumed to be varying linearly along the length (i.e., from Root to Tip). The chord length (c_r) for each element is taken at the middle of each section (Table 3.3). These chord lengths are substituted in the above expressions, which are in turn substituted in Eqs (2.20).

CHAPTER 3

NUMERICAL RESULTS

Based on the formulation given in chapter 2, a computer program is written for the free vibration analysis and flutter analysis of aircraft wing. The results have been validated using a standard package NASTRAN. Further the results of some parametric studies have been presented.

3.1 Free vibration analysis results

3.1.1 Uniform beam

In this section, to ascertain the correctness of the formulation, a bench mark problem of an uniform cantilever beam is solved

Numerical data:

The following properties of the cantilever beam are used for the analysis:

Length = 5m

Width = 2m

Thickness = 0.04m

Young's Modulus of elasticity = E = $70 * 10^9$ N/m^2

Poisson's ration = $\nu = 0.33$

Shear Modulus of rigidity = G = $26.3 * 10^9$ N/m^2

Density of the material = $\rho_s = 2700$ kg/m^3

Density of air = $\rho = 1.225$ kg/m^3

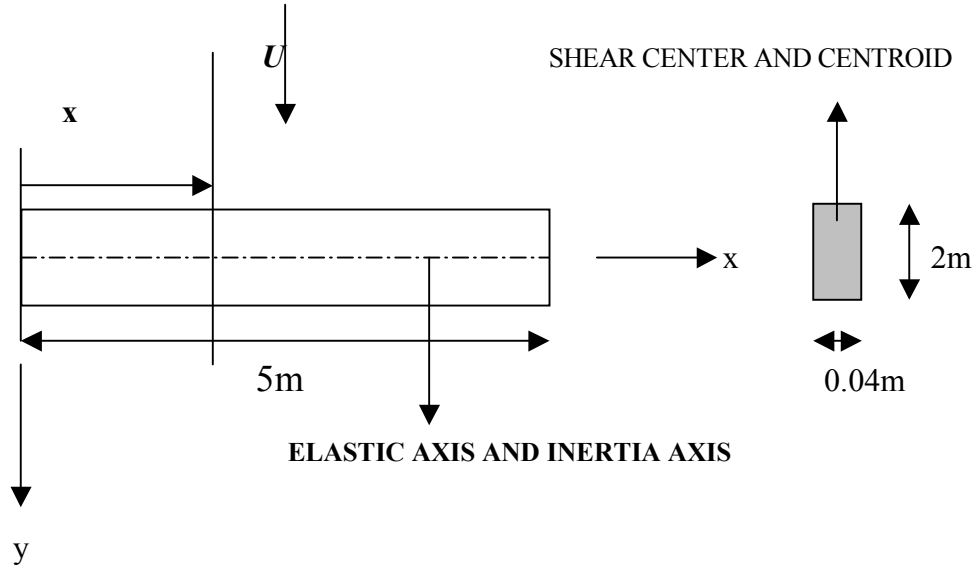

Fig-3.1 (a)

Fig-3.1 (b)

Fig –3.1 (a) Planar view of uniform wing

Fig –3.1 (b) Sectional view of uniform wing

The natural frequencies of typical uniform beam with the properties shown above are as shown in the following Table 3.1

Table 3.1

Natural frequencies of the uniform beam

Type and Mode no.	Program results in Hz	NASTRAN Results in Hz	% Error b/w Program & NASTRAN
1 bending	1.316	1.330	1.05
2 bending	8.404	8.272	-1.59
3 bending	23.533	22.900	-2.76
4 bending	46.115	44.400	-3.86
1 torsion	6.360	6.340	-0.31
2 torsion	19.080	18.880	-1.06
3 torsion	31.798	30.960	-2.70
4 torsion	44.517	43.270	-2.81

3.1.2 The air craft wing

A Typical discretization of the aircraft wing (FE model and Aerodynamic model) are shown in Figs 3.2 and 3.3

Numerical data:

The numerical data used for the actual wing and also for the wings with reduced stiffness parameters are as shown below.

Case (1): ACTUAL WING

Young's Modulus of elasticity = E = $72 * 10^9$ N/m^2

Poisson's ratio = $\nu = 0.3$

Shear Modulus of rigidity = G = $27.69 * 10^9$ N/m^2

Case (2a): WITH REDUCED STIFFNESS PARAMETERS

E* = 0.5E and G* = 0.5G

Young's Modulus of elasticity = E* = $36 * 10^9$ N/m^2

Poisson's ratio = $\nu = 0.3$

Shear Modulus of rigidity = G* = $13.85 * 10^9$ N/m^2

Case (2b): WITH REDUCED STIFFNESS PARAMETERS

E* = 0.1E and G* = 0.1G

Young's Modulus of elasticity = E* = $7.2 * 10^9$ N/m^2

Poisson's ratio = $\nu = 0.3$

Shear Modulus of rigidity = G* = $2.769 * 10^9$ N/m^2

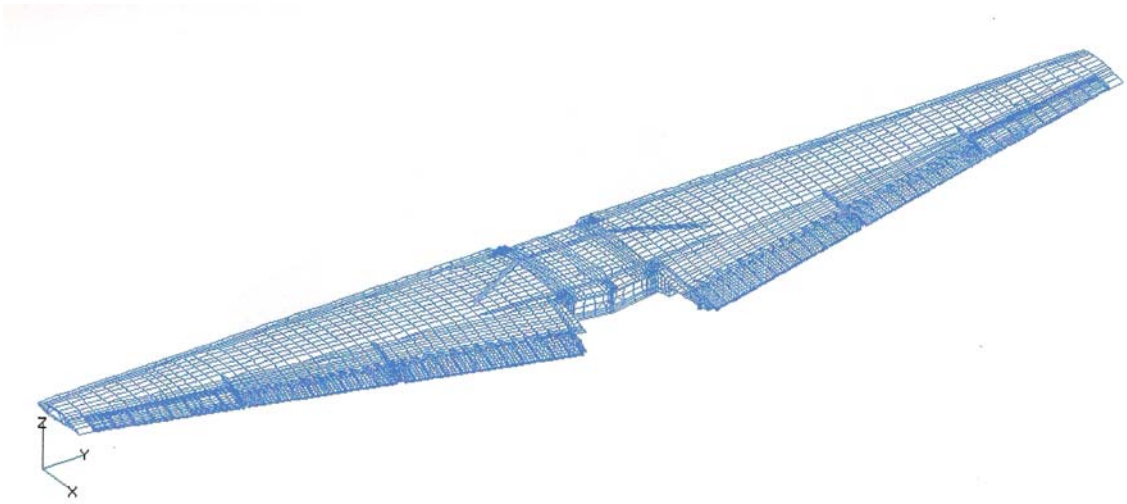

Fig 3.2 An FE model of complete SARAS wing

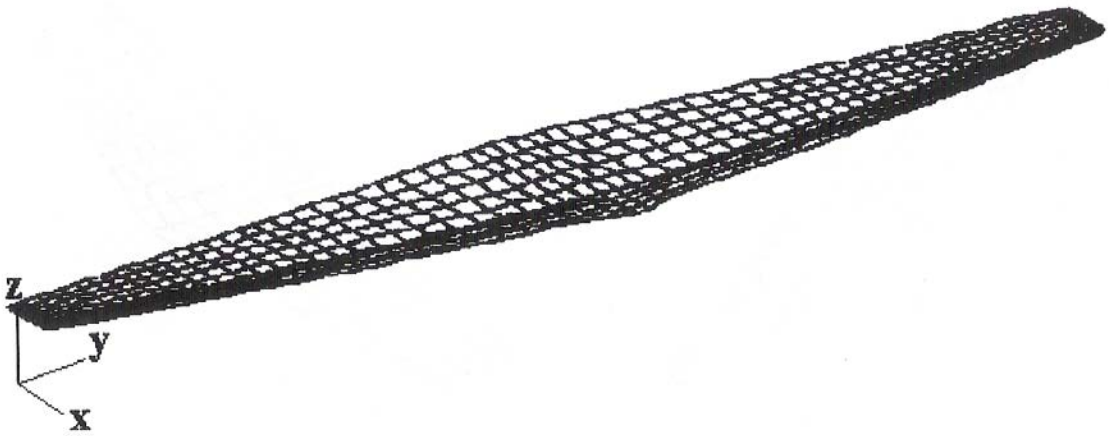

Fig 3.3 Aerodynamic model of SARAS wing

Table 3.2

Mass distribution and mass densities of the beam element

Ref [32] PD ST – 0314

Sl. No.	Ele L in m (l_r)	C/S Area in m^2 x 10^{-6}(A_r)	Density ρ in Kg/m^3 $(\rho_s)_r$	Mass per unit length Kg/m (m_r)
1	0.350	12871.0	9309.30	119.82
2	0.315	12037.0	7803.98	93.94
3	0.285	12318.0	9609.27	118.37
4	0.300	11400.0	9784.31	111.54
5	0.325	15438.0	7654.20	118.16
6	0.315	7348.1	7968.55	58.55
7	0.315	6826.9	49346.43	336.88
8	0.325	6470.2	41645.03	269.45
9	0.325	5314.3	44344.80	235.66
10	0.325	5110.9	40029.30	204.58
11	0.325	4947.1	34392.09	170.14
12	0.325	4817.5	29235.08	14.84
13	0.325	4153.8	26966.23	112.01
14	0.325	3939.4	22792.80	89.79
15	0.325	3455.0	17246.97	59.58
16	0.350	3259.6	9963.28	32.47
17	0.350	3132.6	6385.20	20.00
18	0.300	3153.5	6178.57	19.48
19	0.210	2803.0	9275.77	25.99
20	0.350	2557.7	6660.95	17.04
21	0.370	2009.6	7063.66	14.20
22	0.370	2119.7	6485.07	13.75

Total wing mass = 762.6 kg

Table 3.3

Sectional properties and aerodynamic chord lengths of elements of the wing

Ref [32] PD ST - 0314

Sl. No.	Ele L in m	Izz in m^4 x 10^{-4}	Iyy in m^4 x 10^{-4}	J in m^4 x 10^{-4}	Chord length(m)
1	0.350	4.0477	35.3980	70.3185	2.402
2	0.315	3.2949	29.8140	45.8763	2.326
3	0.285	3.1249	29.5620	25.7400	2.256
4	0.300	2.8388	23.3110	15.0045	2.191
5	0.325	3.7622	23.3330	9.0301	2.120
6	0.315	1.5680	11.6677	7.1700	2.047
7	0.315	1.4159	10.4640	5.6790	1.975
8	0.325	1.2581	9.3388	5.2815	1.902
9	0.325	0.9428	6.8012	4.3770	1.828
10	0.325	0.8215	6.4647	3.8130	1.754
11	0.325	0.7414	6.0293	3.3300	1.680
12	0.325	0.6706	5.4199	2.7525	1.606
13	0.325	0.5127	4.1906	2.3640	1.532
14	0.325	0.4474	3.6573	2.0250	1.458
15	0.325	0.3453	2.8600	1.6335	1.384
16	0.350	0.2958	2.3924	1.3110	1.307
17	0.350	0.2537	2.0252	1.0515	1.227
18	0.300	0.2295	1.8596	0.8730	1.153
19	0.210	0.1901	1.5036	0.7470	1.095
20	0.350	0.1525	1.2544	0.5865	1.031
21	0.370	0.1036	0.7833	0.4125	0.949
22	0.370	0.9409	0.6224	0.2940	0.865

Table 3.4

Shear center position w.r.t. Centroidal axis

Ref [32] PD ST - 0314

Sl. No.	Ele L in m	Z_G in m x 10^{-3}	Y_G in m x 10^{-3}
1	0.350	-355.430	36.300
2	0.315	-432.248	-137.681
3	0.285	-379.560	-199.990
4	0.300	-434.200	-278.100
5	0.325	-161.000	-9.200
6	0.315	-1.648	39.906
7	0.315	-9.040	11.800
8	0.325	-6.333	7.034
9	0.325	-8.275	-3.881
10	0.325	-19.418	-0.664
11	0.325	-18.830	-3.497
12	0.325	-10.425	13.077
13	0.325	-16.588	-4.718
14	0.325	-14.829	-5.609
15	0.325	-6.369	-12.955
16	0.350	-0.028	-10.495
17	0.350	-2.468	8.142
18	0.300	2.517	-8.635
19	0.210	1.100	-7.300
20	0.350	-1.173	-6.608
21	0.370	-0.851	-5.770
22	0.370	-1.952	-5.314

The above numerical data are used for the analysis of the subsonic wing. The wing is visualized as a collection of stepped beam elements, each having its respective properties as shown in the above tables. The natural frequencies obtained for the wing for each case are given below.

Table 3.5

Natural frequencies of the subsonic wing – case (1)

Type and Mode no.	Present analysis results in Hz	Stick model results in Hz Ref [32] Table 4.3 PD ST-0314	3D model results in Hz Ref[32] Table 4.3 PD ST-0314
1 bending	7.331	7.119	7.087
2 bending	21.227	20.786	20.481
3 bending	49.800	48.538	47.781
4 bending	127.767	-	-
1 torsion	57.168	56.500	56.338
2 torsion	123.302	-	-
3 torsion	183.103	-	-
4 torsion	388.522	-	-

Type and Mode no.	%Error b/w program and stick model	%Error b/w program and 3D model
1 bending	2.89	3.33
2 bending	2.07	3.51
3 bending	2.53	4.05
4 bending	-	-
1 torsion	1.17	1.45
2 torsion	-	-
3 torsion	-	-
4 torsion	-	-

Table 3.6

Natural frequencies of the subsonic wing with E*=0.5E – case (2a)

Type and Mode no.	Program results in Hz	NASTRAN results in Hz	% Error b/w Program & NASTRAN
1 bending	5.180	5.03	-2.98
2 bending	15.009	14.60	-2.80
3 bending	35.930	34.10	-5.36
4 bending	103.49	102.20	-1.26
1 torsion	40.420	39.90	-1.30
2 torsion	90.132	92.35	2.40
3 torsion	128.800	129.67	0.67
4 torsion	274.580	266.00	-3.22

Table 3.7

Natural frequencies of the subsonic wing with E*=0.1E – case (2b)

Type and Mode no.	Program results in Hz	NASTRAN results in Hz	% Error b/w Program & NASTRAN
1 bending	2.31	2.24	-3.12
2 bending	6.71	6.50	-3.23
3 bending	16.07	15.20	-5.72
4 bending	44.56	43.32	-2.86
1 torsion	18.07	17.89	-1.00
2 torsion	39.13	38.80	-0.85
3 torsion	57.62	57.99	0.63
4 torsion	122.79	119.15	-3.05

3.2 Flutter analysis

3.2.1 Uniform beam:

The flutter analysis of the uniform rectangular beam is carried out using the modal analysis method. The shear center in the case of uniform section coincides with the centroid of the section. Hence there will be no dynamic coupling in the case of uniform beam.

The Eigen values are obtained for increasing values of velocities. The values obtained are plotted. The velocity v/s the real part of the eigenvalue which is indicative of damping and the velocity v/s the imaginary part of the eigen value which is the frequency in rad/s are plotted from the complex eigen values obtained from the present analysis for different modes. The same graphs are also plotted for the values obtained from NASTRAN for different modes. The graphs plotted are shown in the Figs 3.4 (a) and 3.4 (b)

The flutter speeds obtained from the present analysis and through NASTRAN are shown in the following Table 3.8

Table 3.8

Uniform beam – Flutter results

	Present analysis	NASTRAN
Flutter speed (m/s)	148	170

NASTRAN

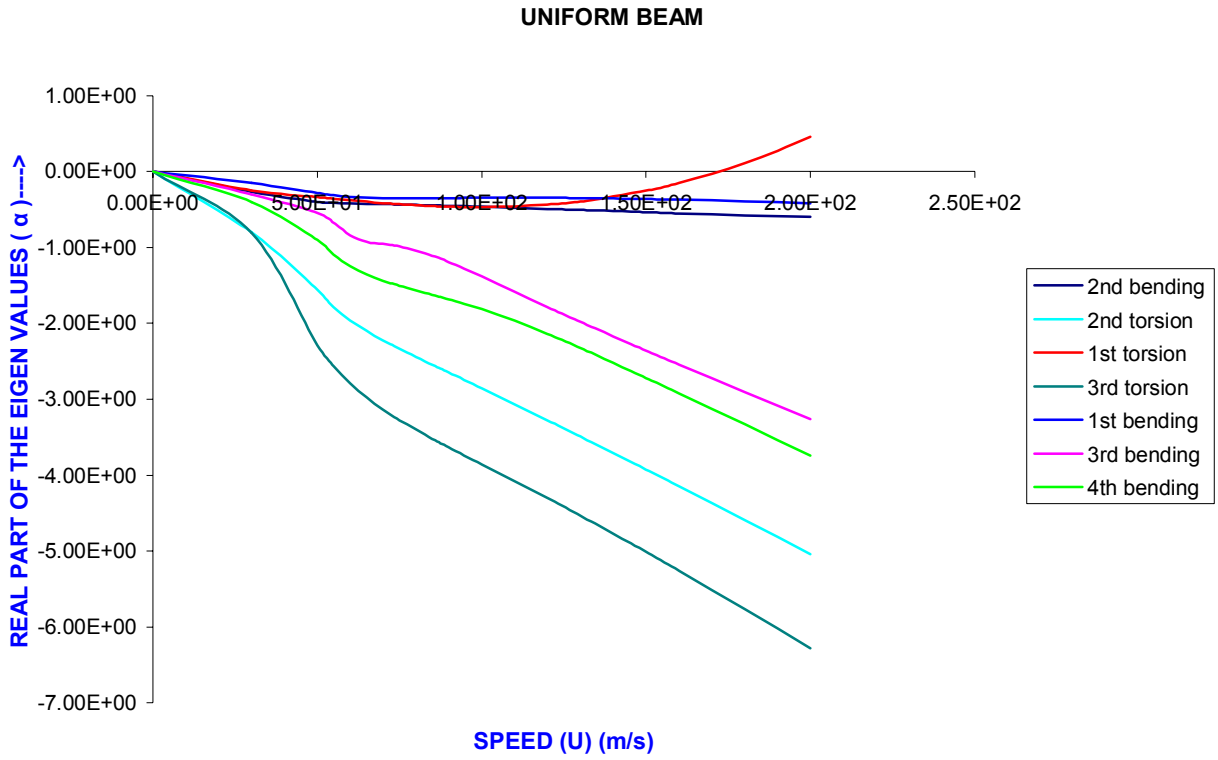

PRESENT ANALYSIS

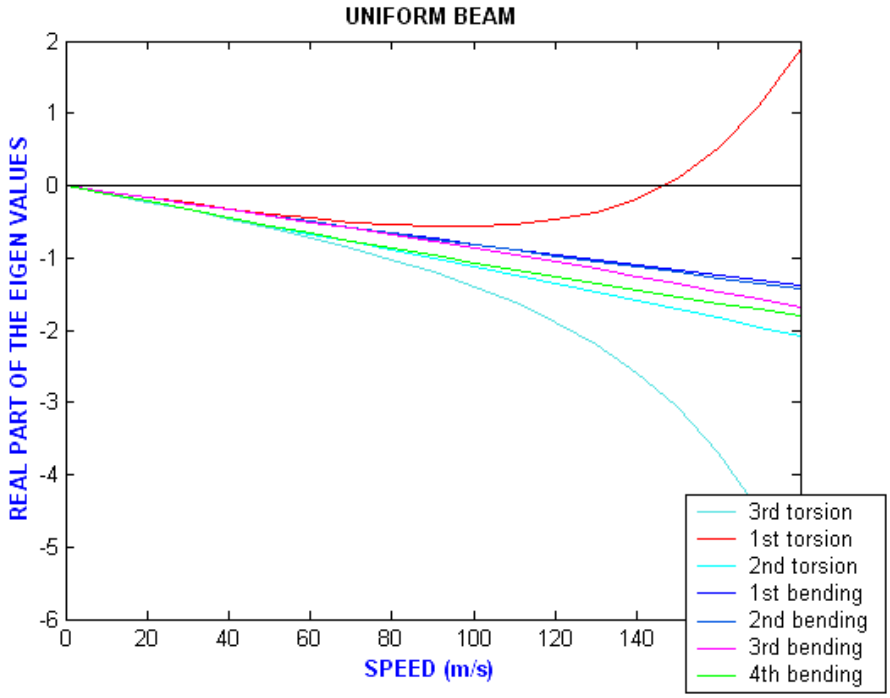

Fig 3.4 (a) Plot of Velocity (U) v/s real part (α) of the eigen value

NASTRAN

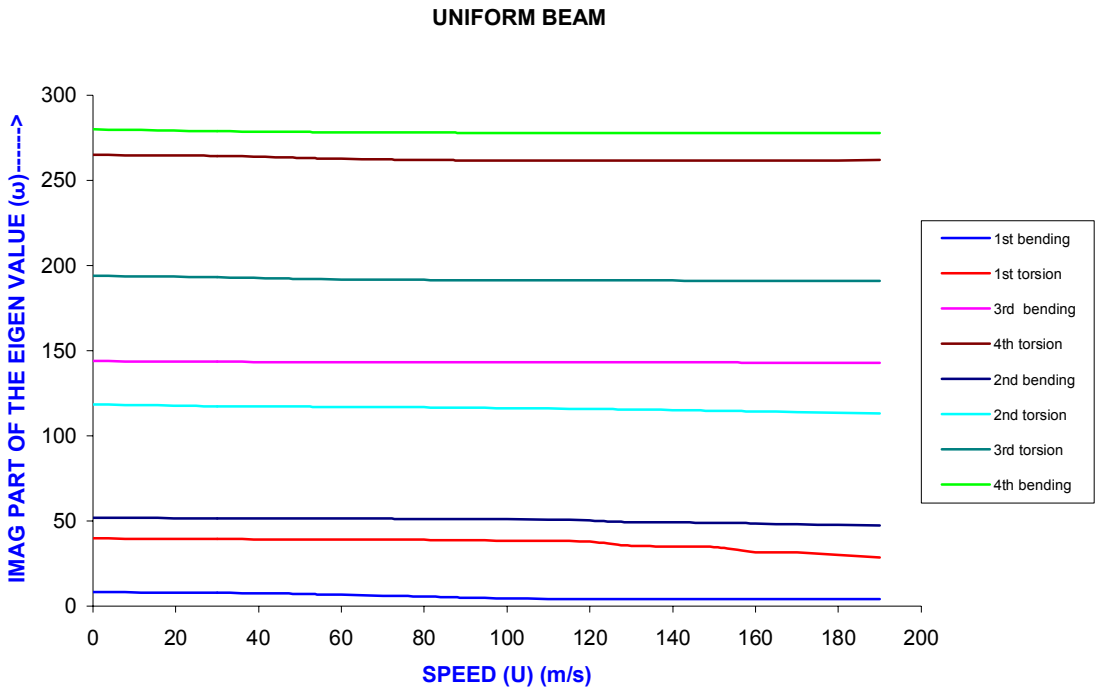

PRESENT ANALYSIS

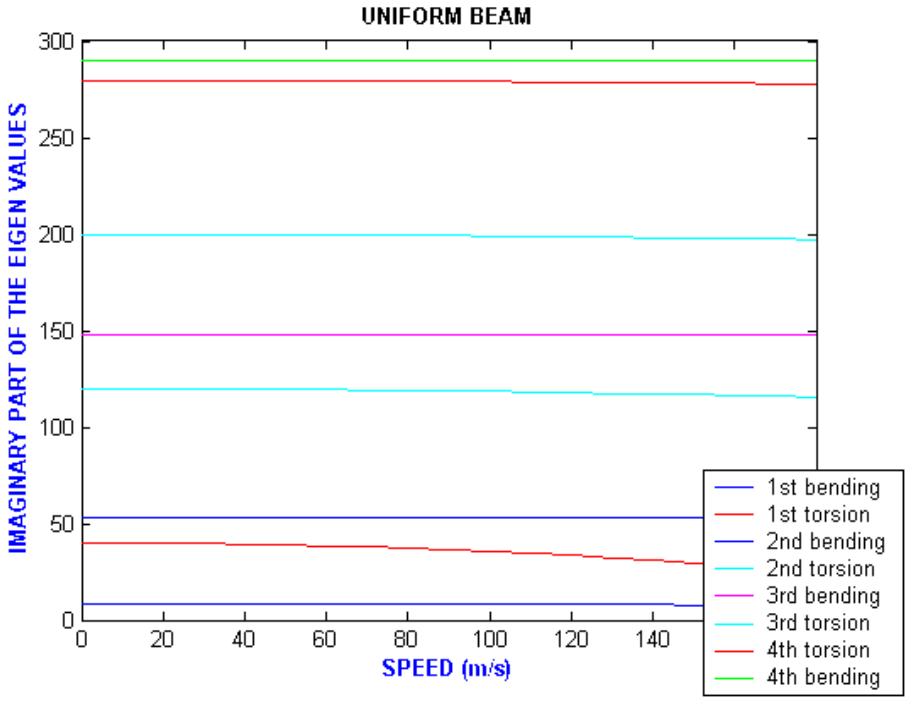

Fig 3.4 (b) Plot of Velocity (U) v/s imaginary part (ω) of the eigen value

3.2.2 Aircraft wing

The flutter analysis of the wing is also carried in the same way with the inclusion of effect of shear center offset. The clean wing modeled as having stepped beam elements is analysed as mentioned before. The velocity v/s the real part of eigen values and velocity v/s the imaginary part of eigen values are plotted from the complex eigen values obtained from the present analysis and also from the NASTRAN.

The velocity v/s damping curves i.e., v-g curves and the velocity v/s frequency curves i.e., v-f curves can also be plotted. The relation between the damping (g) values and eigen values and the relation between the frequency (f) values and eigen values are as given below.

If the eigen value obtained is $\lambda = \alpha+i\omega$, where α is the real part and ω is the imaginary part, then

$$g = \frac{\alpha}{\omega} \text{ x } 2 \quad \text{and} \quad f = \frac{\omega}{2\pi}$$

Hence the v-g and v-f curves can be plotted from the eigen values and the same can also be obtained from NASTRAN.

The velocity v/s Real part and velocity v/s Imaginary part are also plotted for the wing with reduced stiffness parameters. All the graphs obtained are shown below in the Figs 3.5, 3.6, and 3.7

NASTRAN

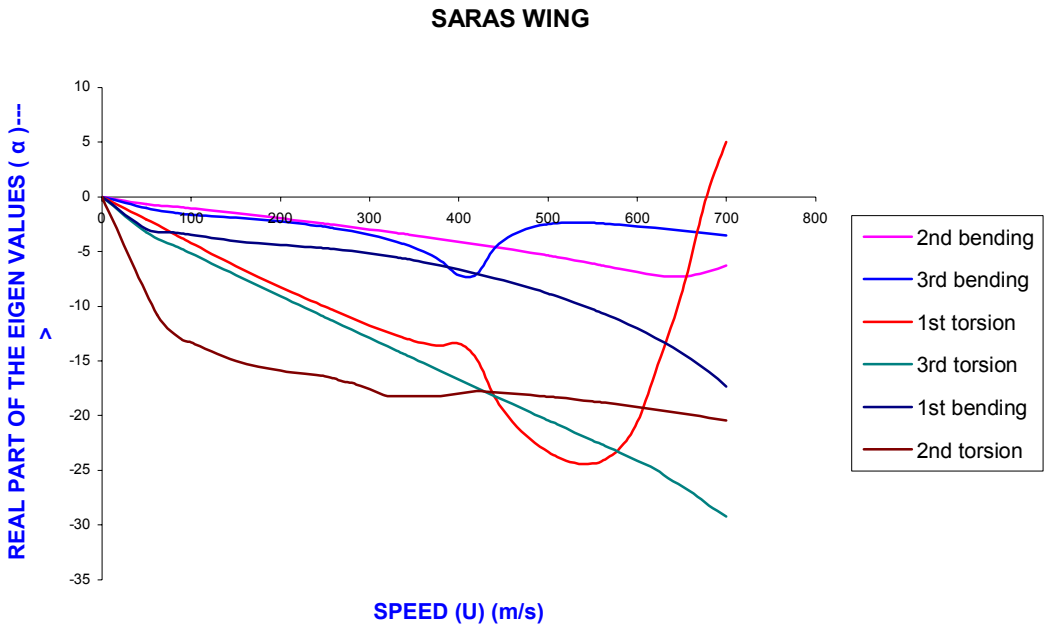

PRESENT ANALYSIS

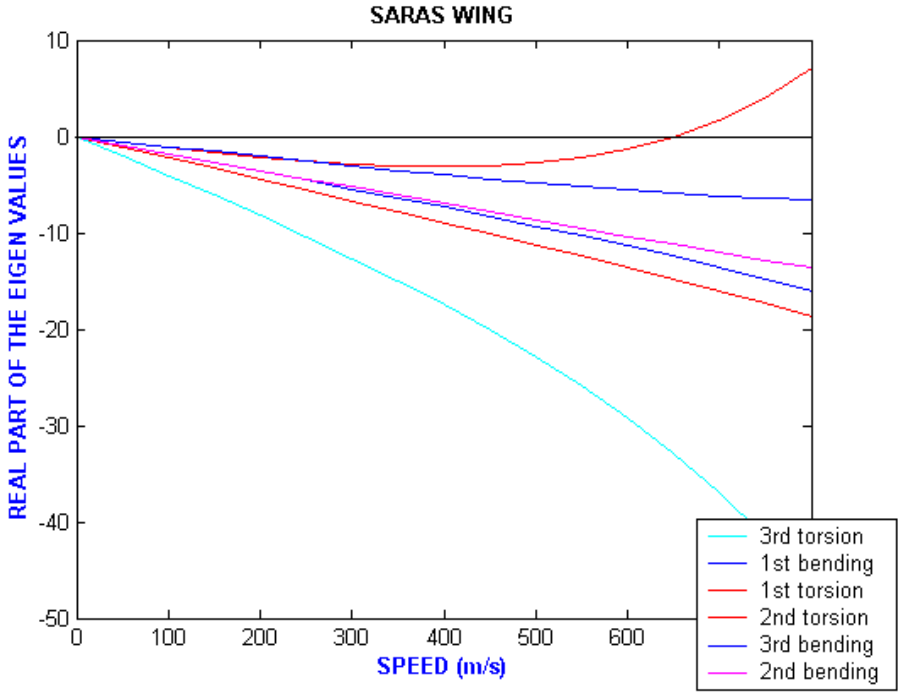

Fig 3.5 (a) Plot of Velocity (U) v/s real part (α) of the eigen value

NASTRAN

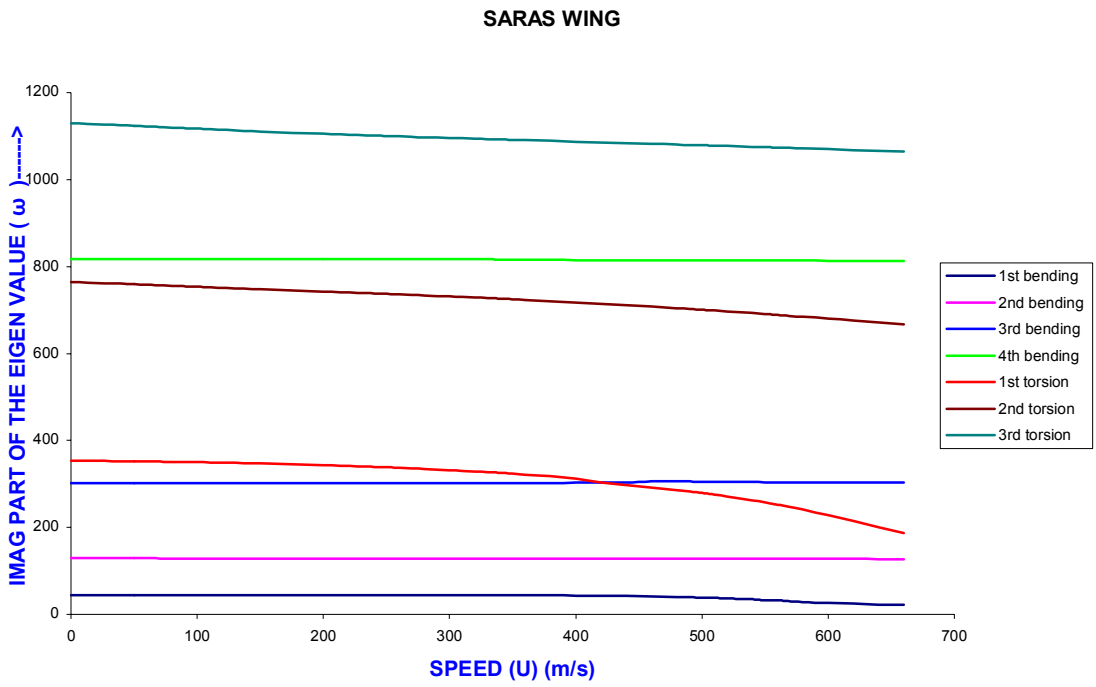

PRESENT ANALYSIS

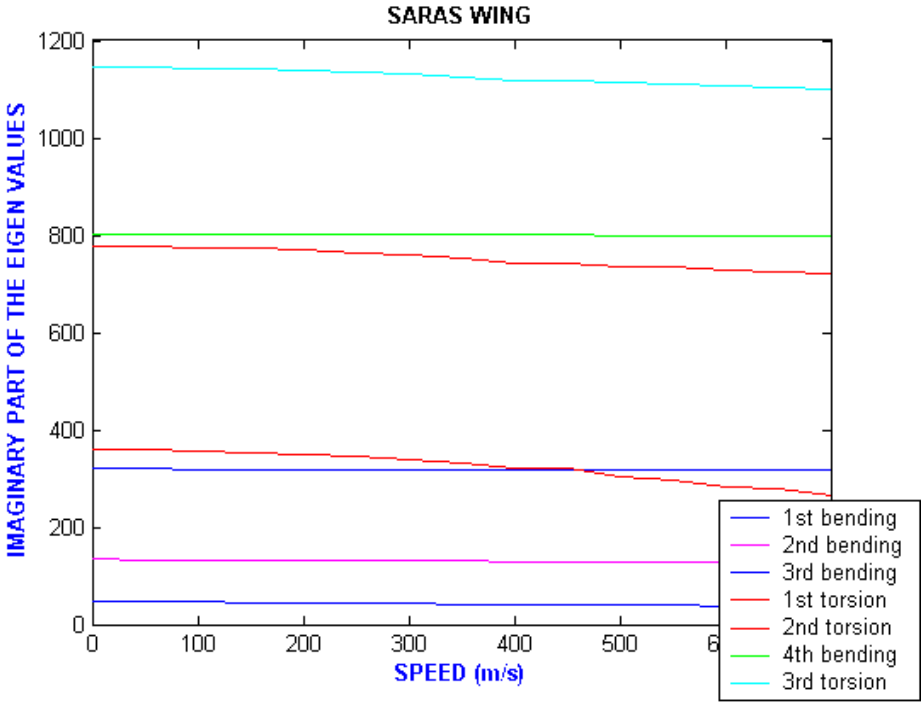

Fig 3.5 (b) Plot of Velocity (U) v/s imaginary part (ω) of the eigen value

NASTRAN

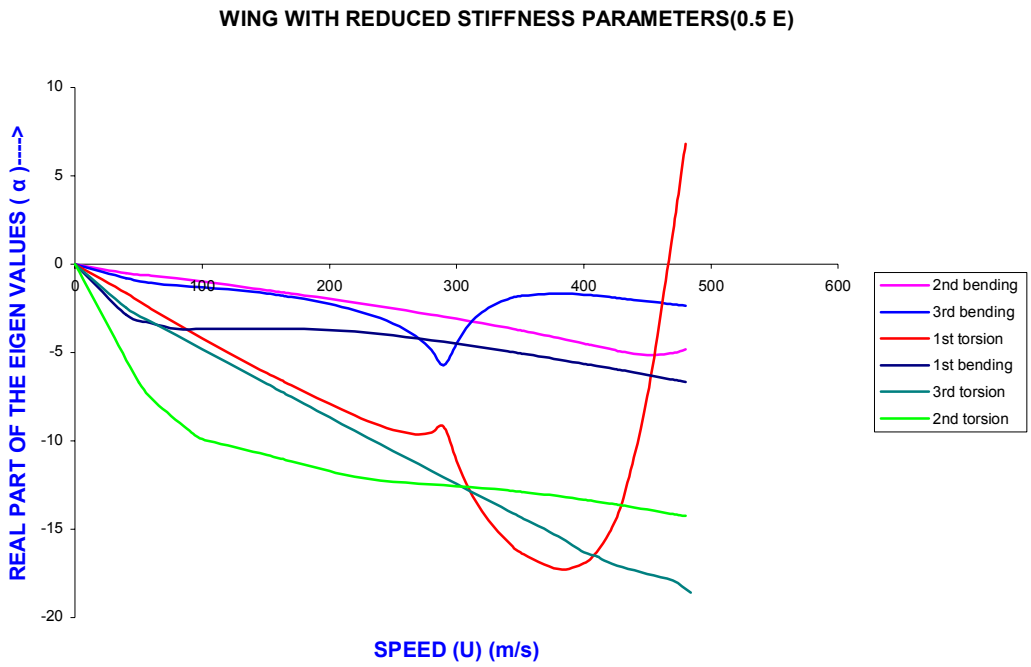

PRESENT ANALYSIS

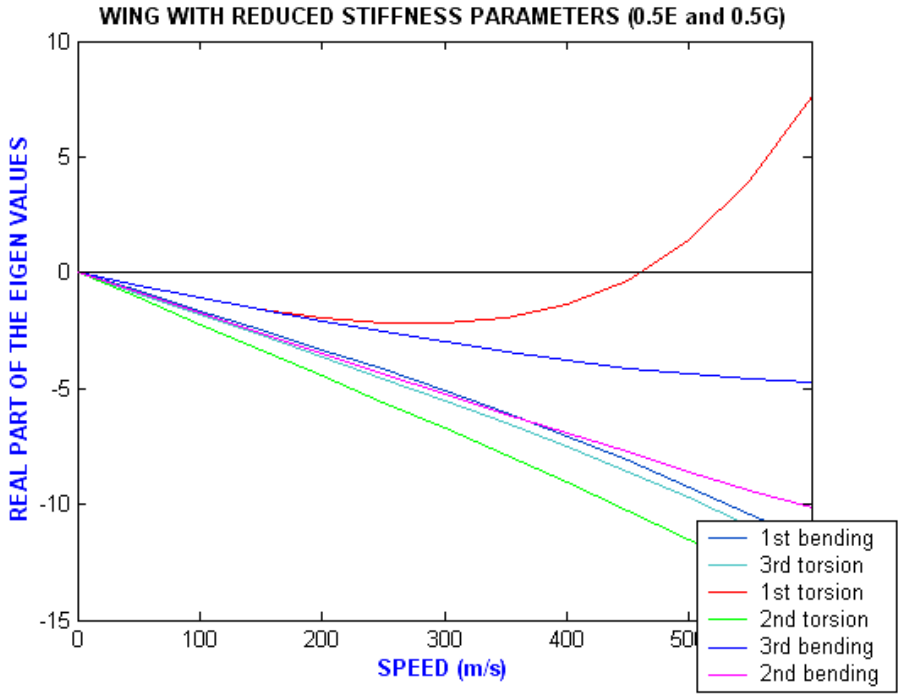

Fig 3.6 (a) Plot of Velocity (U) v/s real part (α) of the eigen value

NASTRAN

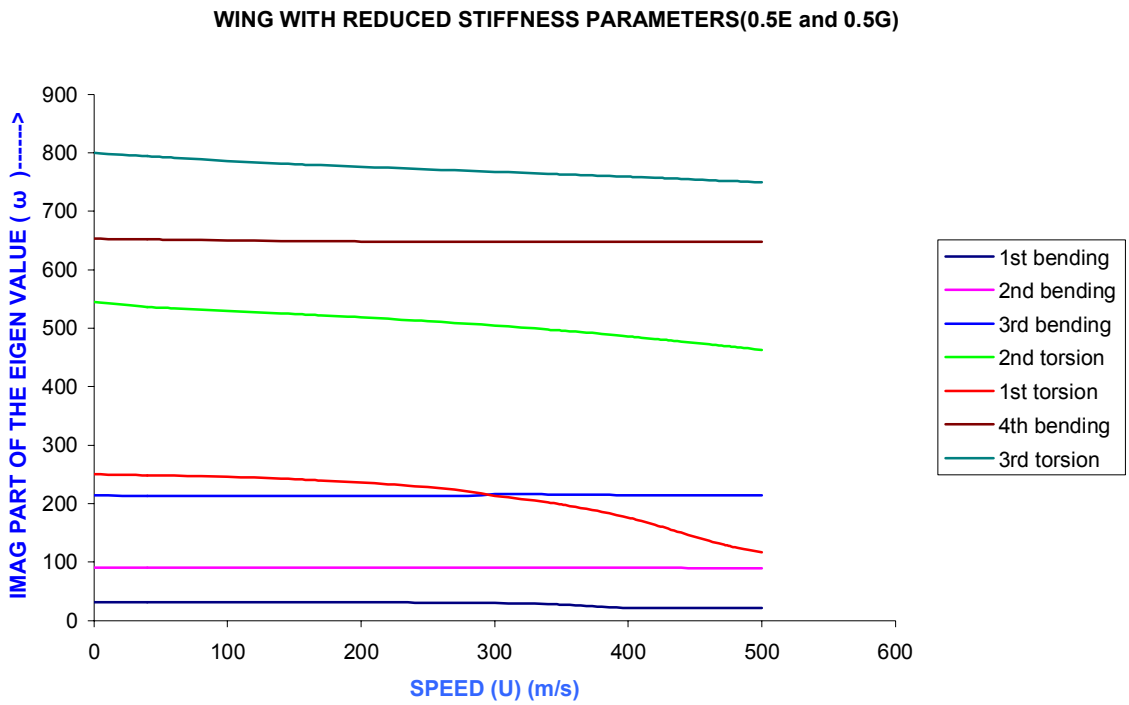

PRESENT ANALYSIS

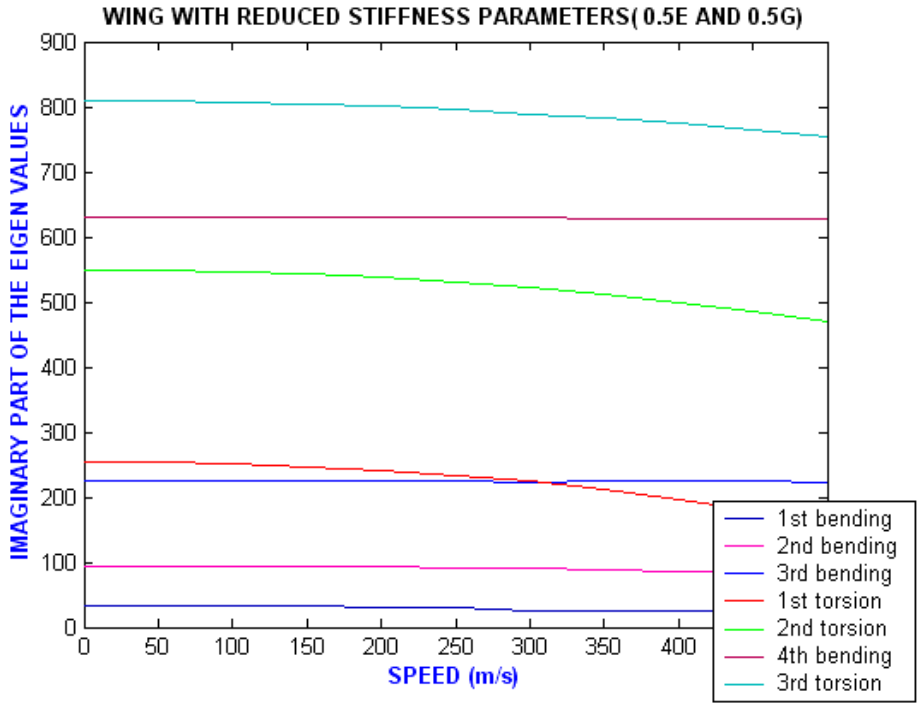

Fig 3.6 (b) Plot of Velocity (U) v/s imaginary part (ω) of the eigen value

NASTRAN

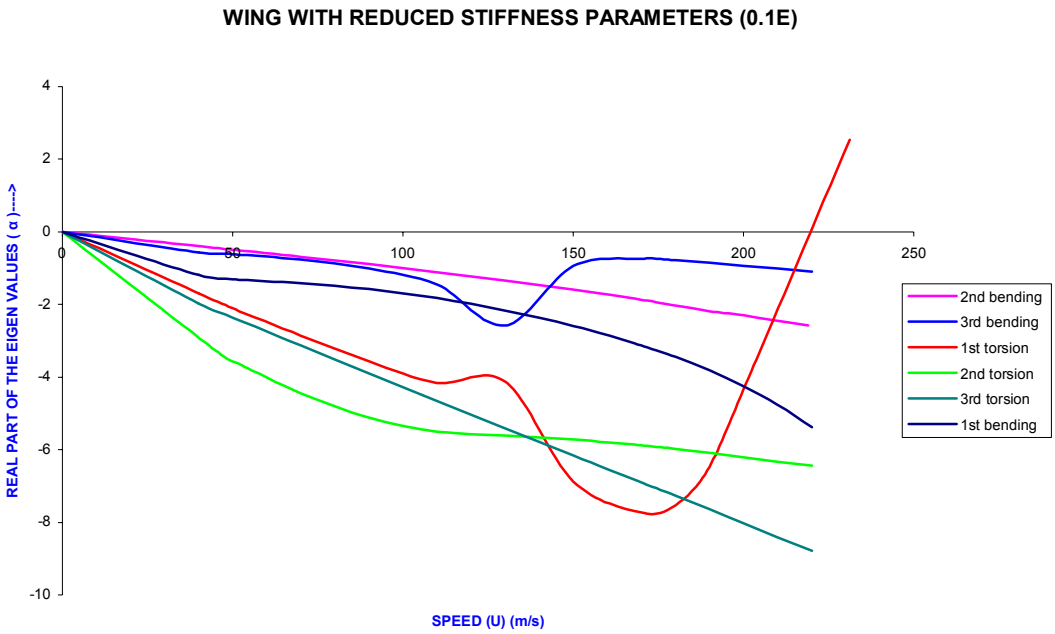

PRESENT ANALYSIS

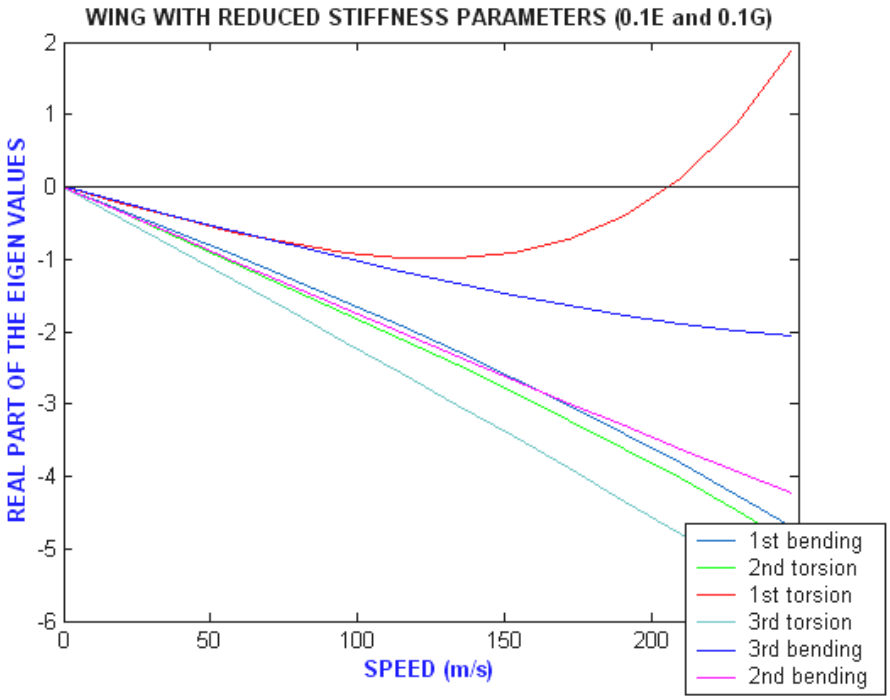

Fig 3.7 (a) Plot of Velocity (U) v/s real part (α) of the eigen value

NASTRAN

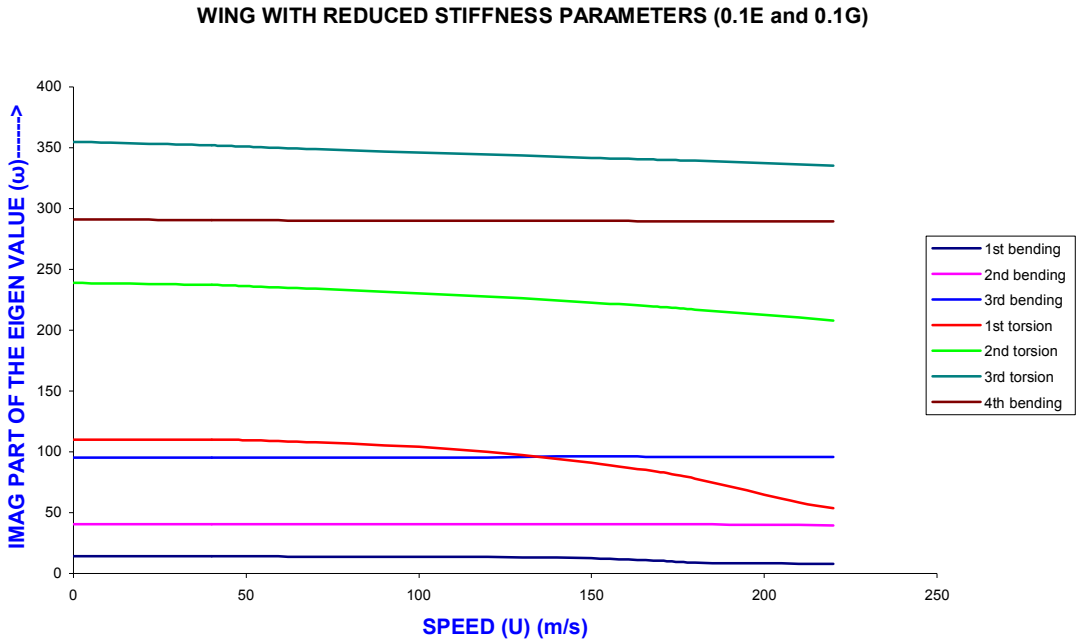

PRESENT ANALYSIS

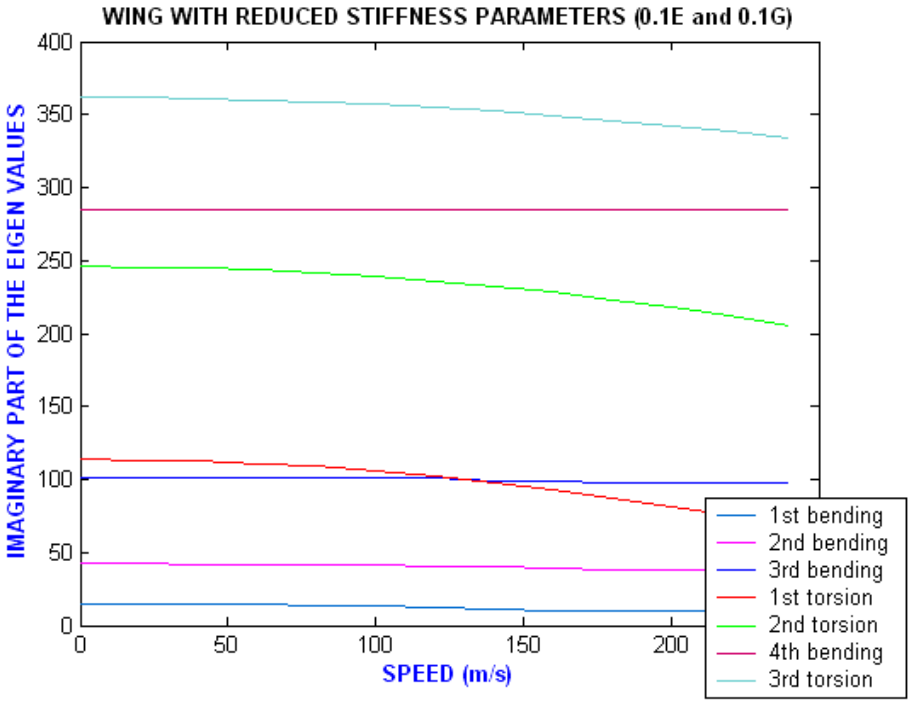

Fig 3.7 (b) Plot of Velocity (U) v/s imaginary part (ω) of the eigen value

The flutter speeds obtained from the graphs for the actual wing and for the wing with reduced stiffness parameters are shown in the following Table 3.9

Table 3.9

Flutter results of the subsonic wing

Flutter speeds (m/s)	Present analysis	NASTRAN
Aircraft wing	650	680
Wing with reduced stiffness parameters (0.5E and 0.5G)	450	470
Wing with reduced stiffness parameters (0.1E and 0.1G)	208	223

CHAPTER 4

CONCLUSIONS

4.1 DISCUSSION OF RESULTS

In the present analysis of subsonic aircraft wing, classical Euler beam model is used. The wing is discretized as a collection of stepped beam elements and is employed for free vibration analysis and the flutter analysis.

The beam model used yields reasonably good results for natural frequencies. The natural frequencies obtained are in good agreement with previously obtained natural frequencies of the clean wing through NASTRAN (Ref [32] PD ST-0314) showing the validity of the present analysis.

For the flutter analysis of the clean wing, the aerodynamic forces are obtained by the quasi-steady subsonic aerodynamic theory. The flutter results obtained by the present method are compared with those obtained from the NASTRAN. The present analysis gives a conservative value of flutter speed as compared to NASTRAN values. The flutter graphs obtained from present analysis and through NASTRAN are shown in the previous chapter. The comparison shows the validity of present method for flutter analysis.

For the clean wing analysis of the SARAS aircraft, the flutter speed is found to be beyond the subsonic regime, i.e., the wing does not flutter in the subsonic flow. Even for the case of flutter speed that exceeds the limit of subsonic regime, agreement of results show that the method adopted is reasonably reliable. Analysis is carried out with reduced stiffness parameters so that the flutter speed falls in the subsonic regime. Again results agree with those from NASTRAN.

4.2 FURTHER SCOPE

1 The present work is limited to the 'clean wing' analysis that doesn't show flutter in the subsonic regime. However it is necessary to check if the wing with control surfaces is prone to subsonic flutter. The present method can be easily extended to determine flutter boundaries of wing with control surfaces

2 The flutter analysis of the T-tail is critical from the point of design. The quasi-steady method can easily be extended to the T-Tail assembly consisting of Horizontal tail, Vertical tail, Rudder and Elevator.

REFERENCES:

1. Lanchester, F.W.: Torsional vibration of the Tail of an Aeroplane. Aeronaut.Research Com.R & M.276, part i (July 1916)

2. Bairstow, L., and A.Fage: Oscillations of the Tail Plane and Body of an Aeroplane in Flight. Aeronaut.Research Com.R & M.276, part ii (July 1916)

3. Blasius,H: Umber Schwingungsercheiningen an Einholmigen Unterflugeln.Z.Flugtech.u.Motorluftschif.16,39-42 (1925)

4. Glauret,H.: The Accelerated Motion of a Cylindrical Body through a Fluid. Aeronaut.Research Com.R & M.1215 (1929)

5. Glauret,H.: The Force and Moment of an Oscillating Aerofoil. Aeronaut.Research Com.R & M.1242 (1929)

6. Theodorsen, Th.: General Theory of Aerodynamic Instability and the Mechanism of Flutter. NACA Rept.496 (1934)

7. Smilg, B.: The Instability of Pitching Oscillations of an Airfoil in Subsonic Incompressible Potential Flow. J.Aeronaut.Sci.16,691-696 (Nov.1949)

8. Cheilik,H., and H.Frissel: Theoretical Criteria for Single Degree of Freedom Flutter at Supersonic Speeds. Cornell Aeronaut.Lab.Rept.CAL-7A (May 1947)

9. Runyan,H.L.,H.J.Cunningham, and C.E.Watkins: Theoretical Investigation of Several Types of Single-Degree-of-Freedom Flutter.J.Aeronaut.Sci.19,101-110, 126 (1952) Comments by K.P.Abichandani and R.M.Rosenberg and author's reply, 215-216; 503-504

10. Cunningham, H.J.: Analysis of Pure-Bending Flutter of a Cantilever Swept Wing and Its Relation to Bending-Torsion Flutter. NACA Tech.Note 2461 (1951)

11. Greidanus, J.H.: Low-Speed Flutter. J.Aeronaut.Sci.16,127-128 (1949)

12. Y.C.Fung, An Introduction to the theory of aero elasticity, John Wiley and sons, Inc

13. E.H.Dowell, Non linear oscillation of a fluttering plate, AIAA J. Vol.4,No.7,July 1996.

14. E.H.Dowell,Theoretical and experimental panel flutter study, AIAA J. Vol.3,No.12,Dec 1995.

15. L.Mirovitch, Elements of Vibration analysis, McGraw Hill Book Co.,1975.

16. D.J.Evins, Modal Testing: Theory and Practice, Research and Study Press Ltd. John Wiley and Sons Inc,1986.

17. R.L.Bisplinghoff and H.Ashley, Aero elasticity; Addison-Wesley Publication 1957.

18. K.F.Alvin and L.D.Paterson, Method for determining minimum order mass and stiffness Matrices from modal test data: AIAA J. Vol.33,No.1,Jan 1995.

19. John Dugundji, Theoretical consideration of Panel flutter at high supersonic Mach No., AIAA J. Vol.4,No.7,July 1966

20. J.B.Kosmatka, Flexure-Torsion behavior of prismatic beam, AIAA J. Vol.31,No.1,Jan 1993.

21. Abott.I.H. and Von Doenhoff, Theory of Wing section, McGraw Hill,Newyork,1949.

22. S.H.R.Eslimy-Islahany and A.J.Sobby, Response of bending torsion coupled beam to deterministic and random loads, J. of Sound and Vibration,195(2),1996.

23. E.Dokumaci, An Exact solution for coupled bending and torsion vibration of uniform beam having single cross section symmetry, J.of Sound and Vibration,119(3),1987.

24. Shyamlal Chatterji, Active stabilization technique of dynamic machine, M.Tech.Thesis, IIT Kanpur, March 1991.

25. W.Wilson, Calculation and Design of Electrical Apparatus, Chapman and Hall Ltd.,1955.

26. Haisler W.E. and Allen D.H., Introduction to Aerospace structural analysis, John Wiley Publication., 1985.

27. Paul Kuhn, Stresses in Aircraft and Shell structure, McGraw Hill Book Co.,Inc.

28. W.T.Thomson, Theory of Vibration with application, George Allen and Unwin, Prantice Hall Publication, 1983.

29. Hurty W.C. and Rubinstein M.F., Dynamics of Structures, Prantice Hall of India Pvt.Ltd.,1967.

30. S.Talukedar, S.Kamle and D.Yadav (1996), Track induced heave pitch dynamics of vehicles with variable section flexible attachment, Vehicle System Dynamics, (Paper to be published)

31. Dowell E.H., D.A.Peters, R.H.Scanlan and F.Sisto, A Modern course in Aeroelasticity, III edition, Kluwer Academic Publishers.

32. Dr. S.Mukherjee, Manju, NAL Project Document, Dynamic characterization SARAS wing and empennage. PD ST-0314

33. L.Mirovitch, Theory of Aero elasticity, McGraw Hill Book Co., 1975.

34. Mario Paz, Structural Dynamics, Theory and Computation,II edition,CBS Publishers and Distributors.

35. Ray W.Clough and Joseph Penzien, Dynamics of Structures, II edition, McGraw-Hill International editions.

36 . Lecture notes by Dr.S.Mukherjee.

37. Dewey H.Hodges and G.Alvin Pierce, Introduction to Structural Dynamics and Aeroelasticity, Cambridge University Press.

APPENDIX I A

FORTRAN code for generation of stiffness, mass and aerodynamic matrices

```
!  AEROELASTIC FLUTTER ANALYSIS OF TAPERED WING(SARAS)
!  QUASI STEADY AERODYNAMIC THEORY IS USED FOR AERODYNAMIC MATRICES
!  NUMERICAL INTEGRATION (TRAPEZOIDAL RULE)
!  IS USED FOR INTEGRATION OF THE MODAL FUNCTIONS

      DIMENSION FUN(51000),SUMKT(10,10),SUMMT(10,10)
      DIMENSION SUMKB(10,10),SUMMB(10,10),SUMMC(10,10)
      DIMENSION STIFF(50,50),FMASS(50,50)
      DIMENSION SUMH2(10,10),SUMH4(10,10)
      DIMENSION SUML1(10,10),SUML2(10,10),SUML3(10,100),SUML4(10,10)
      DIMENSION FHMAT(10,10),FLMAT(10,10)
      DIMENSION TORSIONK(10,10),TORSIONM(10,10)
      DIMENSION BENDINGK(10,10),BENDINGM(10,10)
      DIMENSION COUPLEDM(10,10)
      DIMENSION AEROH2(10,10),AEROH4(10,10)
      DIMENSION AEROL1(10,10),AEROL2(10,10),AEROL3(10,10),AEROL4(10,10)
      DIMENSION STIFF2(50,50),FMASS2(50,50)
      DIMENSION WR(100),WI(100),FMASS1(50,50),STIFF1(50,50)
      DIMENSION anl(10),a(10)

      OPEN(1,FILE='wing.in')
      OPEN(2,FILE='wing.out')

      WRITE (*,*) 'ENTER THE TOTAL LENGTH OF THE BEAM'
      READ (*,*) UL
      WRITE (*,*) 'ENTER THE NUMBER OF DIVISIONS OF THE BEAM'
      READ (*,*) NNN

      DO 9999 N = 1,4
      DO 9999 M = 1,4
      TORSIONK (N, M) = 0.0
      TORSIONM (N, M) = 0.0
      BENDINGK (N, M) = 0.0
      BENDINGM (N, M) = 0.0
      COUPLEDM (N, M) = 0.0
      AEROH2 (N, M) = 0.0
      AEROH4 (N, M) = 0.0
      AEROL1 (N, M) = 0.0
      AEROL2 (N, M) = 0.0
      AEROL3 (N, M) = 0.0
      AEROL4 (N, M) = 0.0
9999  CONTINUE


      DO 5555 III = 1,NNN

!     Reading all the data of each section (material and inertia properties of each section)

      WRITE (*,*) 'ENTER THE LOWER AND UPPER LIMITS OF SECTION',III
      READ (1,*) FL,U
```

```
      WRITE (*,*) 'ENTER THE NUMBER OF DIVISIONS'
      READ (1,*) ND
      WRITE (*,*) 'ENTER THE NUMBER OF MODES'
      READ (1,*) MO
      WRITE (*,*) 'ENTER THE MODULUS OF ELASTICITY'
      READ (1,*) E
      WRITE (*,*) 'ENTER THE MODULUS OF RIGIDITY'
      READ (1,*) G
      WRITE (*,*) 'ENTER THE DENSITY OF THE AIR '
      READ (1,*) RHOA
      WRITE (*,*) 'ENTER THE ASPECT RATIO'
      READ (1,*) AR
      WRITE (*,*) 'ENTER IZZ'
      READ (1,*) FIZZ
      WRITE (*,*) 'ENTER THE CROSS SECTION AREA OF EACH DIVISION'
      READ (1,*) AREA
      WRITE (*,*) 'ENTER THE DENSITY OF THE MATERIAL'
      READ (1,*) RHOM
      WRITE (*,*) 'ENTER J'
      READ (1,*) FJ
      WRITE (*,*) 'ENTER IXX'
      READ (1,*) FIXX
      WRITE (*,*) 'ENTER THE SHEAR CENTER OFFSET'
      READ (1,*) YTHETA
      WRITE (*,*) 'ENTER THE CHORD LENGTH OF THE ELEMNET'
      READ (1,*) CHORD

      PI=4.0*ATAN (1.0)
!-------------------------------------------------------------------------------
      DO 500 N=1,MO
      DO 500 M=1,MO
      H=(U-FL)/ND
      N1=ND+1
      S1=0.0
      S2=0.0
      S3=0.0
      S4=0.0
      S5=0.0
      S6=0.0
      S7=0.0
      S8=0.0
      S9=0.0
      S10=0.0
      S11=0.0

      PI=4.0*ATAN(1.0)

!     stiffness matrix for torsion -SUMKT(N,M)
!     TORSIONK(N,M) - summation of integrals SUMKT(N,M) of each section
      DO 50 I=1,N1
      X=FL+(I-1)*H
      CALL KT(N,M,X,UL,G,FJ,FKT)
      FUN(I)=FKT
      S1=2.0*FUN(I)+S1
50    CONTINUE
      S1=S1-FUN(1)-FUN(N1)
      SUMKT(N,M) = S1*H/2.0
      TORSIONK(N,M) = TORSIONK(N,M) + SUMKT(N,M)
```

```
!       mass matrix for torsion -SUMMT(N,M)
!       TORSIONM(N,M) - summation of integrals SUMMT(N,M) of each section

        DO 60 I=1,N1
        X=FL+(I-1)*H
        CALL MT(N,M,X,UL,RHOM,FIXX,FFMT)
        FUN(I)=FFMT
        S2=2.0*FUN(I)+S2
60      CONTINUE
        S2=S2-FUN(1)-FUN(N1)
        SUMMT(N,M) = S2*H/2.0
        TORSIONM(N,M) = TORSIONM(N,M) + SUMMT(N,M)

!       stiffness matrix for bending
        DO 70 I=1,N1
        X=FL+(I-1)*H
        CALL KB(N,M,X,UL,FIZZ,E,FKB)
        FUN(I)=FKB
        S3=2.0*FUN(I)+S3
70      CONTINUE
        S3=S3-FUN(1)-FUN(N1)
        SUMKB(N,M) = S3*H/2.0
        BENDINGK(N,M) = BENDINGK(N,M) + SUMKB(N,M)

!       mass matrix for bending
        DO 80 I=1,N1
        X=FL+(I-1)*H
        CALL MB(N,M,X,UL,RHOM,AREA,FMB)
        FUN(I)=FMB
        S4=2.0*FUN(I)+S4
80      CONTINUE
        S4=S4-FUN(1)-FUN(N1)
        SUMMB(N,M) = S4*H/2.0
        BENDINGM(N,M) = BENDINGM(N,M) + SUMMB(N,M)
!       coupled mass matrix
        DO 90 I=1,N1
        X=FL+(I-1)*H
        CALL MC(N,M,X,UL,AREA,YTHETA,FMC)
        FUN(I)=FMC
        S5=2.0*FUN(I)+S5
90      CONTINUE
        S5=S5-FUN(1)-FUN(N1)
        SUMMC(N,M) = S5*H/2.0
        COUPLEDM(N,M) = COUPLEDM(N,M) + SUMMC(N,M)

!       aerodynamic matrices

        DO 200 I=1,N1
        X=FL+(I-1)*H
        CALL HH2(N,M,X,UL,FH2)
        FUN(I)=FH2
        S6=2.0*FUN(I)+S6
200     CONTINUE
        S6=S6-FUN(1)-FUN(N1)
        SUMH2(N,M) = ((RHOA*PI)*S6*H/2.0)
        AEROH2(N,M) = AEROH2(N,M) + SUMH2(N,M)
```

```
      DO 210 I=1,N1
      X=FL+(I-1)*H
      CALL HH4(N,M,X,UL,YTHETA,FH4)
      FUN(I)=FH4
      S7=2.0*FUN(I)+S7
210   CONTINUE
      S7=S7-FUN(1)-FUN(N1)
      SUMH4(N,M) = ((RHOA*PI)*S7*H/2.0)
      AEROH4(N,M) = AEROH4(N,M) + SUMH4(N,M)

      DO 220 I=1,N1
      X=FL+(I-1)*H
      CALL LL1(N,M,X,UL,FFL1)
      FUN(I)=FFL1
      S8=2.0*FUN(I)+S8
220   CONTINUE
      S8=S8-FUN(1)-FUN(N1)
      SUML1(N,M) = RHOA*PI * S8*H/2.0
      AEROL1(N,M) = AEROL1(N,M) + SUML1(N,M)

      DO 230 I=1,N1
      X=FL+(I-1)*H
      CALL LL2(N,M,X,UL,YTHETA,FFL2)
      FUN(I)=FFL2
      S9=2.0*FUN(I)+S9
230   CONTINUE
      S9=S9-FUN(1)-FUN(N1)
      SUML2(N,M) = RHOA * PI * S9*H/2.0
      AEROL2(N,M) = AEROL2(N,M) + SUML2(N,M)

      DO 240 I=1,N1
      X=FL+(I-1)*H
      CALL LL3(N,M,X,UL,YTHETA,FFL3)
      FUN(I)=FFL3
      S10=2.0*FUN(I)+S10
240   CONTINUE
      S10=S10-FUN(1)-FUN(N1)
      SUML3(N,M) = -( (RHOA * PI ) * S10*H/2.0)
      AEROL3(N,M) = AEROL3(N,M) + SUML3(N,M)

      DO 250 I=1,N1
      X=FL+(I-1)*H
      CALL LL4(N,M,X,UL,DCL,YTHETA,FFL4)
      FUN(I)=FFL4
      S11=2.0*FUN(I)+S11
250   CONTINUE
      S11=S11-FUN(1)-FUN(N1)
      SUML4(N,M) = (0.5*RHOA)*S11*H/2.0
      AEROL4(N,M) = AEROL4(N,M) + SUML4(N,M)


500           CONTINUE
```

```
      WRITE (2,*) '"STIFFNESS MATRIX FOR PURE TORSION"'
      DO 111 N=1,MO
      DO 110 M=1,MO
      WRITE (2,15) TORSIONK(N,M)
110   CONTINUE
      WRITE (2,*)
111   CONTINUE


      WRITE (2,*) '"MASS MATRIX FOR PURE TORSION"'
      DO 121 N=1,MO
      DO 120 M=1,MO
      WRITE (2,15) TORSIONM(N,M)
120   CONTINUE
      WRITE (2,*)
121   CONTINUE

      WRITE (2,*) '"STIFFNESS MATRIX FOR PURE BENDING"'
      DO 131 N=1,MO
      DO 130 M=1,MO
      WRITE (2,15) BENDINGK(N,M)
130   CONTINUE
      WRITE (2,*)
131   CONTINUE

      WRITE (2,*) '"MASS MATRIX FOR PURE BENDING"'
      DO 141 N=1,MO
      DO 140 M=1,MO
      WRITE (2,15) BENDINGM(N,M)
140   CONTINUE
      WRITE (2,*)
141   CONTINUE

      WRITE (2,*) '"COUPLED MASS MATRIX"'
      DO 151 N=1,MO
      DO 150 M=1,MO
      WRITE (2,15) COUPLEDM(N,M)
150   CONTINUE
      WRITE (2,*)
151   CONTINUE

      WRITE (2,*) '"H2 MATRIX"'
      DO 301 N=1,MO
      DO 300 M=1,MO
      WRITE (2,16) AEROH2(N,M)
300   CONTINUE
      WRITE (2,*)
301   CONTINUE

      WRITE (2,*) '"H4 MATRIX"'
      DO 311 N=1,MO
      DO 310 M=1,MO
      WRITE (2,16) AEROH4(N,M)
310   CONTINUE
311   CONTINUE
```

```
      WRITE (2,*) '"L1 MATRIX"'
      DO 321 N=1,MO
      DO 320 M=1,MO
      WRITE (2,16) AEROL1(N,M)
320   CONTINUE
      WRITE (2,*)
321   CONTINUE


      WRITE (2,*) '"L2 MATRIX"'
      DO 331 N=1,MO
      DO 330 M=1,MO
      WRITE (2,16) AEROL2(N,M)
330   CONTINUE
      WRITE (2,*)
331   CONTINUE

      WRITE (2,*) '"L3 MATRIX"'
      DO 341 N=1,MO
      DO 340 M=1,MO
      WRITE (2,16) AEROL3(N,M)
340   CONTINUE
      WRITE (2,*)
341   CONTINUE

      WRITE (2,*) '"L4 MATRIX"'
      DO 351 N=1,MO
      DO 350 M=1,MO
      WRITE (2,16) AEROL4(N,M)
350   CONTINUE
      WRITE (2,*)
351   CONTINUE

15    FORMAT (F15.4,$)
16    FORMAT (F19.15,$)

5555  CONTINUE

      STOP
      END
```

```
!-------------------------------------------------------------------------------------------------------
!       SUBROUTINES FOR THE COMPUTATION OF MODAL FUNCTIONS
!-------------------------------------------------------------------------------------------------------

!       STIFFNESS MATRIX FOR BENDING
        SUBROUTINE KB(N,M,X,U,FIZZ,E,FKB)

        DIMENSION anl(10),a(10)

        PI=4.0*ATAN(1.0)

        anl(1) =  1.8753
        anl(2) =  4.6941
        anl(3) =  7.8547
        anl(4) = 10.9953

        SIG1 = ( COS(anl(N)) + COSH(anl(N)) ) / ( SIN(anl(N)) +SINH(anl(N)) )
        SIG2 = ( COS(anl(M)) + COSH(anl(M)) ) / ( SIN(anl(M)) +SINH(anl(M)) )

        a(1) =  1.8753/U
        a(2) =  4.6941/U
        a(3) =  7.8547/U
        a(4) = 10.9953/U

        FK1 = (COSH(a(N)*X)+COS(a(N)*X)) - (SIG1 * (SINH(a(N)*X) + SIN(a(N)*X)))
        FK2 = (COSH(a(M)*X)+COS(a(M)*X)) - (SIG2 * (SINH(a(M)*X) + SIN(a(M)*X)))

        AA = (a(N))**2
        BB = (a(M))**2

        FKB = E * FIZZ * (FK1*FK2) * (AA) * (BB)

        RETURN
        END
!-----------------------------------------------------------------------
!       MASS MATRIX FOR BENDING
        SUBROUTINE MB(N,M,X,U,RHOM,AREA,FMB)

        DIMENSION anl(10),a(10)

        PI=4.0*ATAN(1.0)

        anl(1) =  1.8753
        anl(2) =  4.6941
        anl(3) =  7.8547
        anl(4) = 10.9953

        SIG1 = ( COS(anl(N)) + COSH(anl(N)) ) / ( SIN(anl(N)) +SINH(anl(N)) )
        SIG2 = ( COS(anl(M)) + COSH(anl(M)) ) / ( SIN(anl(M)) +SINH(anl(M)) )

        a(1) =  1.8753/U
        a(2) =  4.6941/U
        a(3) =  7.8547/U
        a(4) = 10.9953/U


        FM1 = (COSH(a(N)*X)-COS(a(N)*X)) - (SIG1 * (SINH(a(N)*X) - SIN(a(N)*X)))
        FM2 = (COSH(a(M)*X)-COS(a(M)*X)) - (SIG2 * (SINH(a(M)*X) - SIN(a(M)*X)))
```

```
      FMB = (RHOM*AREA) * FM1 * FM2

      RETURN
      END
!-----------------------------------------------------------------------
!     STIFFNESS MATRIX FOR TORSION
      SUBROUTINE KT(N,M,X,U,G,FJ,FKT)

      PI=4.0*ATAN(1.0)

      A = ((2.0*N-1)*PI*X)/(2.0*U)
      B = ((2.0*M-1)*PI*X)/(2.0*U)

      C = (2.0*N-1)*PI/(2.0*U)
      D = (2.0*M-1)*PI/(2.0*U)

      FKT =  G * FJ * (COS(A)*COS(B)) * C * D

      RETURN
      END
!-----------------------------------------------------------------------
!     MASS MATRIX FOR TORSION

      SUBROUTINE MT(N,M,X,U,RHOM,FIXX,FFMT)

      PI=4.0*ATAN(1.0)

      A = ((2*N-1)*PI*X)/(2*U)
      B = ((2*M-1)*PI*X)/(2*U)

      FFMT = (RHOM*FIXX) * (SIN(A) * SIN(B))

      RETURN
      END
!-----------------------------------------------------------------------
!     COUPLED MASS MATRIX (IF THERE IS SHEAR CENTER OFFSET)
      SUBROUTINE MC(N,M,X,U,AREA,YTHETA,FMC)
      DIMENSION anl(10),a(10)

      PI=4.0*ATAN(1.0)

      anl(1) =  1.8753
      anl(2) =  4.6941
      anl(3) =  7.8547
      anl(4) = 10.9953

      SIG1 = ( COS(anl(N)) + COSH(anl(N)) ) / ( SIN(anl(N)) +SINH(anl(N)) )

      a(1) =  1.8753/U
      a(2) =  4.6941/U
      a(3) =  7.8547/U
      a(4) = 10.9953/U

      B = ((2*M-1)*PI*X)/(2*U)

      FM1 = (COSH(a(N)*X)-COS(a(N)*X)) - (SIG1 * (SINH(a(N)*X) - SIN(a(N)*X)))
      FM2 =   SIN(B)

      FMC = (RHOM*AREA) * YTHETA * FM1*FM2
```

```
      RETURN
      END

!-----------------------------------------------------------------------
!     AERO DYNAMIC MATRICES

      SUBROUTINE HH2(N,M,X,U,CHORD,FH2)
      DIMENSION anl(10),a(10)

      PI=4.0*ATAN(1.0)

      anl(1) =  1.8753
      anl(2) =  4.6941
      anl(3) =  7.8547
      anl(4) = 10.9953

      SIG1 = ( COS(anl(N))+COSH(anl(N)) ) / ( SIN(anl(N))+SINH(anl(N)) )

      a(1) =  1.8753/U
      a(2) =  4.6941/U
      a(3) =  7.8547/U
      a(4) = 10.9953/U

      B = ((2*M-1)*PI*X)/(2*U)

      FH21=(COSH(a(N)*X)-COS(a(N)*X)) - (SIG1 * (SINH(a(N)*X) - SIN(a(N)*X)))
      FH22=SIN(B)


      FH2 = CHORD*FH21*FH22

      RETURN
      END

!-----------------------------------------------------------------------

      SUBROUTINE HH4(N,M,X,U,YTHETA,CHORD,FH4)

      PI=4.0*ATAN(1.0)

      A = ((2*N-1)*PI*X)/(2*U)
      B = ((2*M-1)*PI*X)/(2*U)


      Y0 = (CHORD/2.0) - YTHETA

      FH4 =  ( (CHORD**2.0) * (Y0/CHORD-0.25) * (SIN(A) * SIN(B)) )

      RETURN
      END
```

```
      SUBROUTINE LL1(N,M,X,U,CHORD,FFL1)
      DIMENSION anl(10),a(10)

      PI=4.0*ATAN(1.0)

      anl(1) =  1.8753
      anl(2) =  4.6941
      anl(3) =  7.8547
      anl(4) = 10.9953

      SIG1 = ( COS(anl(N)) + COSH(anl(N)) ) / ( SIN(anl(N)) +SINH(anl(N)) )
      SIG2 = ( COS(anl(M)) + COSH(anl(M)) ) / ( SIN(anl(M)) +SINH(anl(M)) )

      a(1) =  1.8753/U
      a(2) =  4.6941/U
      a(3) =  7.8547/U
      a(4) = 10.9953/U

      FL11= (COSH(a(N)*X)-COS(a(N)*X)) - (SIG1 * (SINH(a(N)*X) - SIN(a(N)*X)))
      FL12= (COSH(a(M)*X)-COS(a(M)*X)) - (SIG2 * (SINH(a(M)*X) - SIN(a(M)*X)))


      FFL1 = CHORD*(FL11*FL12)

      RETURN
      END
!-----------------------------------------------------------------------
      SUBROUTINE LL2(N,M,X,U,YTHETA,CHORD,FFL2)
      DIMENSION anl(10),a(10)

      PI=4.0*ATAN(1.0)

      anl(1) =  1.8753
      anl(2) =  4.6941
      anl(3) =  7.8547
      anl(4) = 10.9953

      SIG1 = ( COS(anl(N)) + COSH(anl(N)) ) / ( SIN(anl(N)) +SINH(anl(N)) )

      a(1) =  1.8753/U
      a(2) =  4.6941/U
      a(3) =  7.8547/U
      a(4) = 10.9953/U

      B = ((2*M-1)*PI*X)/(2*U)

      FL21= (COSH(a(N)*X)-COS(a(N)*X)) - (SIG1 * (SINH(a(N)*X) - SIN(a(N)*X)))
      FL22=   SIN(B)

      Y0 = (CHORD/2.0) - YTHETA

      FFL2 = ( (CHORD**2) * (0.75-Y0/CHORD) * FL21*FL22 )
      RETURN
      END
```

```
      SUBROUTINE LL3(N,M,X,U,YTHETA,CHORD,FFL3)
      DIMENSION anl(10),a(10)

      PI=4.0*ATAN(1.0)

      anl(1) =  1.8753
      anl(2) =  4.6941
      anl(3) =  7.8547
      anl(4) = 10.9953

      SIG2 = ( COS(anl(M)) + COSH(anl(M)) ) / ( SIN(anl(M)) +SINH(anl(M)) )

      a(1) =  1.8753/U
      a(2) =  4.6941/U
      a(3) =  7.8547/U
      a(4) = 10.9953/U

      B = ((2*N-1)*PI*X)/(2*U)

      FL31=  SIN(B)
      FL32= (COSH(a(M)*X)-COS(a(M)*X)) - (SIG2 * (SINH(a(M)*X) - SIN(a(M)*X)))

      Y0 = (CHORD/2.0) - YTHETA

      FFL3 = ( (CHORD**2) * (Y0/CHORD-0.25)  * FL31*FL32 )

      RETURN
      END
!-----------------------------------------------------------------------
      SUBROUTINE LL4(N,M,X,U,DCL,YTHETA,CHORD,FFL4)

      PI=4.0*ATAN(1.0)

      A = ((2*N-1)*PI*X)/(2*U)
      B = ((2*M-1)*PI*X)/(2*U)

      Y0 = (CHORD/2.0) - YTHETA

    FFL4 =  ( (CHORD**3)  * ((PI/8.0) - ( (Y0/CHORD-0.25) * (0.75-Y0/CHORD)*(2.0*PI) ))
                * (SIN(A) * SIN(B)) )

      RETURN
      END
!-----------------------------------------------------------------------
```

APPENDIX I B

MATLAB code for the eigen value analysis

```
%       kb = bending stiffness matrix
%       mb = bending mass matrix
%       kt = torsional stiffness matrix
%       mt = torsional mass matrix
%       mc coupled mass matrix
%       h1,h2,h3,h4,l1,l2,l3,l4 = aerodynamic matrices
%      the above matrices have to be input here for the eigen value analysis



       kc = zeros(4,4)

%       "H1 MATRIX"
        h1 = zeros(4,4);

 %      "H3 MATRIX"
        h3 = zeros(4,4);

%      stiffness matrix
        stiff1 = [kb;kc];
        stiff2 = [kc;kt];
        stiff = [stiff1,stiff2];
         ss = stiff

%      mass matrix
          mass1 = [mb;mc];
          mass2 = [mc;mt];
          mass = [mass1,mass2];
           mm = mass

%      aerodynamic matrices

          aeroh1 = [h1;h3];
          aeroh2 = [h2;h4];
          hh = [aeroh1,aeroh2];

          aerol1 = [l1;l3];
          aerol2 = [l2;l4];
          ll = [aerol1,aerol2];
```

```
%       n = number of modes
        n = 4


%         finding eigenvalues for different speeds

          u=-50.0;
          for nn=1:17
             u = u + 50.0
             uu(nn) =  u ;

             a1 = zeros(2*n);
             a2 = eye(2*n);
             a3 = -( ss + (uu(nn)^2 * (hh)) );
             a4 = -uu(nn)*(ll);

             aa1 = [a1,a2];
             aa2 = [a3,a4];
             aa  = [aa1;aa2];


             b1 = eye(2*n);
             b2 = zeros(2*n);
             b3 = zeros(2*n);
             b4 = mm;


             bb1 = [b1,b2];
             bb2 = [b3,b4];
             bb  = [bb1;bb2];

            [v2,d2] = eig(aa,bb,'qz');

             dd = (sort(diag(d2)))

          end


%         the eigen values obtained are complex .
%         the eigen values obtained will not be in order which has to be sorted and the
graphs can be plotted  using the “plot” command
```